DESIGN AND CONSTRUCT MULTIPLE LINEAR FACETS INTEGRATED COLLECTOR STORAGE SOLAR WATER HEATER (ICSSWH)

FON CHUN YIN

A project report submitted in partial fulfilment of the requirements for the award of the degree of Bachelor of Engineering (Hons) Industrial Engineering

Faculty of Engineering and Green Technology
Universiti Tunku Abdul Rahman

January 2018

DECLARATION

I hereby declare that this project report is based on my original work except for citations and quotations which have been duly acknowledged. I also declare that it has not been previously and concurrently submitted for any other degree or award at UTAR or other institutions.

Signature : ___________________________

Name : ___________________________

ID No. : ___________________________

Date : ___________________________

APPROVAL FOR SUBMISSION

I certify that this project report entitled **"DESIGN AND CONSTRUCT MULTIPLE LINEAR FACETS INTEGRATED COLLECTOR STORAGE SOLAR WATER HEATER (ICSSWH)"** was prepared by **FON CHUN YIN** has met the required standard for submission in partial fulfilment of the requirements for the award of Bachelor of Engineering (Hons) Industrial Engineering at Universiti Tunku Abdul Rahman.

Approved by,

Signature : _________________________

Supervisor : Dr. Tan Ming Hui

Date : _________________________

Specially dedicated to

my beloved parents and friends.

ACKNOWLEDGEMENTS

I would like to thank everyone who had contributed to the successful completion of this project. I would like to express my gratitude to my research supervisor, Dr. Tan Ming Hui for his invaluable advice, guidance and his enormous patience throughout the development of the research.

In addition, I would also like to express my gratitude to my loving parent and friends who had helped and given me encouragement throughout this project.

Moreover, I would like to express my gratitude to Mr. Mohd. Syahrul Husni bin Hassan for his assistance in the construction of the prototype.

DESIGN AND CONSTRUCT MULTIPLE LINEAR FACETS INTEGRATED COLLECTOR STORAGE SOLAR WATER HEATER (ICSSWH)

ABSTRACT

Solar energy is a free, clean and safe form of energy source which can be obtained repetitively and persistently from the natural environment. The solar energy can be harvested and converted into thermal energy by solar water heater for domestic usage. Solar water heater is a well-established technology for water heating in many countries around the world. There are many different solar water heater systems and solar collectors available in the market due to the needs of different locations and applications. However, there are some weaknesses for all these solar water heater systems and solar collectors. In this project, a simple, high efficiency and easy fabricated multiple linear facets integrated collector storage solar water heater (ICSSWH) is constructed. A totally new design solar collector, multiple linear facets collector is designed by using trigonometry approach and ray tracing simulation is carried out to validate the design. Besides that, the mechanical structure of multiple linear facets ICSSWH is designed by using SolidWorks and then constructed in UTAR. The experimental study and cost analysis of the multiple linear facets ICSSWH are carried out and presented in detailed in this project. Lastly, the multiple linear facets ICSSWH has proved that it can achieved the theoretical maximum efficiency of 65.27% and highest water temperature of 83.0°C with a payback period of 4.23 years.

TABLE OF CONTENTS

LIST OF TABLES

LIST OF FIGURES

LIST OF SYMBOLS / ABBREVIATIONS

a	distance from the intersection point of reflected ray and tank surface to the end point of first slanted mirror, °
A	the total area of the entry aperture of the multiple linear facets ICSSWH, m^2
A_p	area exposed to irradiance, m^2
b	distance from the midpoint of the tank to the end point of first slanted mirror, °
c_m	y-intercept of slanted mirror
c_r	y-intercept of reflected ray
c_{water}	specific heat capacity of water, J/(kg·°C)
g	gravitational acceleration, m/s^{-2}
G	solar irradiance, W/m^2
i	interest rate
I_{ave}	average global solar irradiance, W/m^2
j	inflation rate of the fuel
m	mass of water, kg
m_m	gradient of slanted mirror
m_r	gradient of reflected ray
n_{pay}	payback period, year
P_ann	annual saved fuel cost, RM/year
P_u	power output of a collector, W
Q_{col}	collected thermal energy, J
$Q_{incident}$	total amount of solar energy radiated on the entry aperture, J
r	radius of tank
R_L	radioactive resistance, K/W

S_{total}	total manufacturing cost of the multiple linear facets ICSSWH system, RM
T_a	ambient temperature, °C
$T_{ave, amb}$	average ambient temperature over an interval time, °C
$T_{ave, heating}$	average water temperature in the storage tank over the period of heating for an interval time, °C
$T_{f, amb}$	final ambient temperature over the interval of time, °C
$T_{f, heating}$	final heating temperature of the water, °C
$T_{i, amb}$	initial ambient temperature over the interval of time, °C
$T_{i, heating}$	initial heating temperature of the water, °C
T_p	plate temperature, °C
$\bar{T}_f$	mean fluid temperature, °C
U_L	coefficient of overall heat loss, W/m^{2}K
Δt	time interval, s
α_p	fraction of flux being absorbed
δ	declination angle, °
l_{base}	length of base mirror
l_m	length of slanted mirror
η_c	efficiency of a collector
η_{sp}	capture efficiency
η_{pf}	transfer efficiency
τ_{cov}	transmittance of transparent cover
θ_t	angle between center line of the tank and tank's radius which perpendicular to reflected ray, °
$\theta_{m\ (new)}$	angle of the next mirror from base mirror, °
θ_T	angle of reflection of the 90° angle incident ray from the new mirror, °
θ_r	angle between the reflected ray and a straight line which from the midpoint of the tank to the end point of first slanted mirror, °
θ_z	depression angle from the end point of first slanted mirror to the midpoint of the tank, °

CAD	computer aided design
GHI	global horizontal irradiance, W/m^2
GUI	graphic user interface
ICSSWH	integrated collector storage solar water heater
IGES	initial graphics exchange specification

LIST OF APPENDICES

CHAPTER 1

INTRODUCTION

1.1 Overview

Solar energy is one of the renewable energy which can be obtained repetitively and persistently from the natural environment (Twidell and Weir, 2015). According to Devanarayanan and Murugavel (2014), solar energy is a free, clean and safe form of energy source compared to fossil fuels; hence it is the most prosperous energy source in the world. The average power density of solar radiation reaching Earth's atmosphere is 1366 W/m^2, which also known as solar constant. Based on some calculations, the total power of solar radiation reaching the Earth is about 1.73×10^{17} W, and hence it is about 5.46×10^{24} J or 5,460,000 EJ of energy reaching the Earth annually. The annual energy consumption of the entire world is quite small when compared with it in which the annual energy consumption is just about 500 EJ or 0.01% of the annual solar energy. But not all the solar radiation which falls on the Earth's atmosphere can reaches the ground, about 30% of it will be reflected into space, 20% of it will be absorbed by clouds and molecules in the air and more important is that only one quarter of the Earth's surface is ground. Even only 10% of it is utilizable, it already able to power the whole world with only 0.1% of it (Chen, 2011).

According to Kumar and Rosen (2010), solar water heater is a well-established technology for water heating in many countries around the world. There are three different designs of the solar water heater such as natural convection (passive), forced circulation (active) and also integrated collector-storage (ICS). Due to the needs of different locations and applications, there are many different solar water heater designs available in the market in which some are simple and some are complicated (Kumar and Rosen, 2010). Flat-plate, evacuated-tube and compound parabolic concentrator are the most common collectors which used in these solar water systems.

In most of the cold climate countries such as Canada, the forced circulation type of solar water heater with antifreeze would be the best choice for them as it has a large variation in the air temperature and freezing conditions. However, the price for this system is relatively high and has payback periods up to 20 years or more. On the other hand, natural convection or thermosyphon solar water heater is more suitable for the developing countries due to its simple design and grid power independence (Kumar and Rosen, 2010).

For an integrated collector storage solar water heater (ICSSWH), the solar collector and the water storage tanks are combined into one unit. In comparison with other designs of solar water heater, the ICSSWH is simpler in design and operation as well as lower in costs. Nonetheless, there are also some weaknesses for the ICSSWH system. The heat loss of the ICSSWH system is high when compared with other solar water heaters due to the storage tank cannot be thermally well-insulated as it is act as the receiver of the system. As a result, the thermal performance of the ICSSWH system is relatively poor, especially during night time or non-collecting periods (Devanarayanan and Murugavel, 2014). Hence, the improvement studies of the thermal performance of the ICSSWH system have been done by researchers, especially for overnight applications. Based on the study done by Souliotis et al. (2013), double glazing able to reduce the thermal losses of the ICSSWH system significantly, during the day and night. Other than that, Kumar and Rosen (2010) suggested that corrugated absorber surface with small corrugation depth is a better choice compared to a plane absorber surface for ICSSWH system in which it has a higher characteristics length that can influence the coefficient of convective heat transfer from absorber to water. Moreover, Kumar and Rosen (2011) also proposed that ICSSWH system with an extended storage tank which is well-insulated will improve the heat retaining capability of the whole system.

1.2 Problem Statements

According to Kumar and Rosen (2010), ICSSWH system can be considered as one of the simplest designs solar water heater as it is simple, efficient and cost-effective in converting solar energy into useful thermal energy. Many studies have been carried out in order to improve the efficiency of ICSSWH system as well as to reduce the overall costs.

One of the factors that will affect the overall performance of the ICSSWH is the type of solar collector used. Currently, flat-plate, evacuated-tube and compound parabolic concentrator are the collectors that widely used in solar water heater systems. However, there are some weaknesses for each of these collectors. For flat-plate and evacuated-tube collectors, they are non-concentrating so the concentration ratio for them will be smaller or equals to 1 ($CR \leq 1$). On the other hand, CPC able to attain concentration ratio of more than 1 ($CR \geq 1$) but with its complicated geometric due to its curvature, it is hard to fabricate and the imperfection of its symmetrical design may occurred during the manufacturing process, and hence reduce its effectiveness.

In conclusion, it is a need to design and develop a totally new design of collector in which it can attain concentration ratio of more than one with simpler optical geometry and manufacturing process which have good thermal performance.

1.3 Aims and Objectives

The objectives of the thesis are shown as following:

i) To design the optical geometry of the multiple linear facets Integrated Collector Storage Solar Water Heater.
ii) To construct the mechanical structure of the multiple linear facets Integrated Collector Storage Solar Water Heater.

iii) To evaluate the performance of the multiple linear facets Integrated Collector Storage Solar Water Heater.

CHAPTER 2

LITERATURE REVIEW

2.1 Position of the Earth and the Sun

According to Twidell and Weir (2015), it is crucial to take into account the position of the sun at different time period of the year at different places when designing for a solar energy generating system which including the angle of the sun's height (solar altitude or elevation which measured in degrees) and the azimuth (direction facing away from true north which also measured in degrees). Besides that, the sun in the tropics and equatorial zones is overhead for most of the time with slight difference between the seasons which means that a solar collector does not need to be tilted to any great extent. On the other hand, it is essential to tilt the collector which away from these zones towards the equator where facing north in southern, and facing south in the northern hemisphere (Laughton, 2010).

The Earth orbits around the Sun once per year with the direction of its axis remains fixed in space, at an angle, $\delta = 23.45°$ away from the normal to the plane of revolution as shown in the Figure 2.1. The angle between the Sun and the equatorial plane is known as the declination angle, δ which relating to the seasonal changes. As a result, the δ will changes smoothly from $+\delta = +23.45°$ at midsummer in the northern hemisphere, to $-\delta = -23.45°$ at midwinter in the northern hemisphere (Twidell and Weir, 2015).

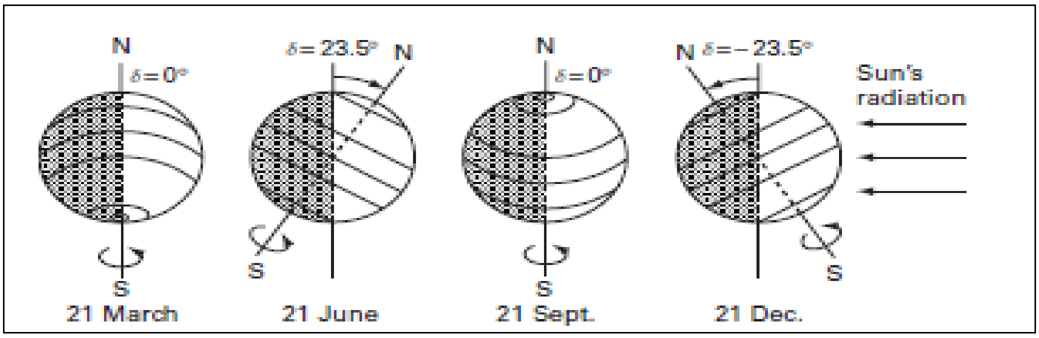

Figure 2.1: The Sun Declination, δ Varies Throughout the Year (Twidell and Weir,2015)

According to Twidell and Weir (2015), the amount of energy harvest will be probably the maximum if a solar collector can track the sun in order to ensure that the incident angle to the direct solar radiation is always perpendicular. However, the cost for the sun-tracking system is expensive and the operating and maintenance costs also higher than the fixed mounted collectors (Twidell and Weir, 2015).

2.2 Solar Water Heating (SWH) System

Solar water heating (SWH) system is used to harvest thermal energy from the sun to heat up water which will be used for clothes washing, domestic purposes in urban and rural areas as well as the needs in industry, agriculture and business (Twidell and Weir, 2015). According to Laughton (2010), a significant period of development in solar water heating in 1970s was due to the dramatically growth in oil prices and the further development was led by the aim to preserve the non-renewable resources such as coal, oil and natural gas as well as to reduce the carbon dioxide (CO_2) emissions. Based on the studies by Union of Concerned Scientists, it can fulfill 50 - 80% of a typical household's hot water needs with the installation of a SWH system and it may meet 100% of their hot water needs if it is in sunny and hot areas such as Hawaii. There are more than 200 million households in this world are using solar water heating system with more than half in China in order to fulfil their hot water needs for daily activities (Twidell and Weir, 2015). With this, it will reduce the usage of electricity and hence cut down the demand on the fossil fuel resources. At the same time, it will indirectly enhance the environment by decreasing the emissions of greenhouse gasses which will lead to water and air pollution as well as the global warming. The working mechanism of a SWH system is very simple where a moving fluid will pass through a dark surface area that exposed to sunlight which used to heat up the fluid. This can be either an active system where water is being heated up directly, or a heat transfer fluid likes glycol or water mixture is used and then brought into some form of heat exchanger is known as an indirect system (Shelke et al., 2014). There are 2 different types of SWH system which are active system and passive system.

2.2.1 Active System

Electric pumps, valves and controllers are used in this kind of system in order to circulate water or different kind of heat-transfer fluids through the collectors. Therefore, active system can also be known as forced circulation system. Although it is more complex or even more expensive than other system but it carry some advantages (Shelke et al., 2014):-

- No restrictions of where to place the storage tanks.
- Able to have more control over the system.
- More efficient.
- Drainback tanks can be used.

For the active system, it can be further separated into Open-loop (direct) or Closed-loop (indirect) system.

2.2.1.1 Open-loop (Direct) Active System

Normally, this direct active system is usually used in a warmer or non-freezing climates so the water is directly circulated through the collectors and back into the storage tanks as shown in Figure 2.2. According to Union of Concerned Scientists, this system can be worked with photovoltaic or differential controllers for the controlling of circulating pump’s operation.

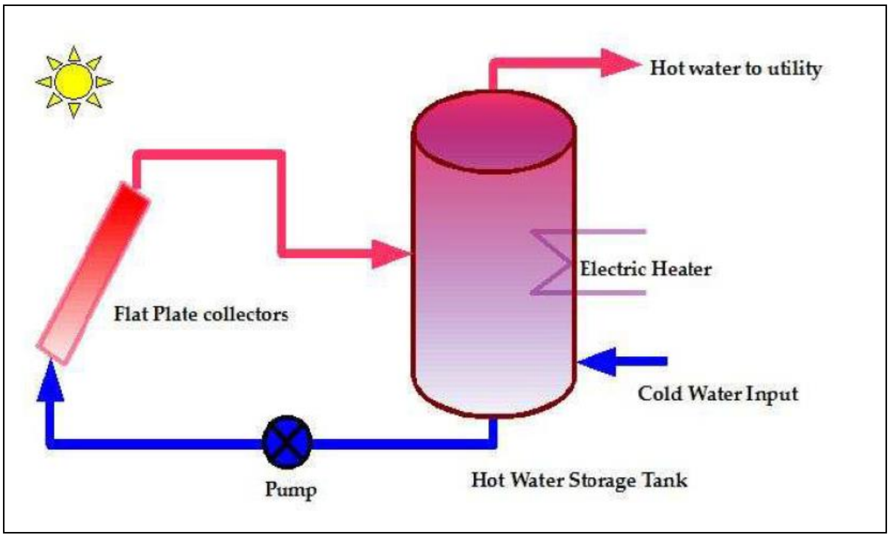

Figure 2.2: Open-loop (Direct) Active System (Johari et al., 2012)

2.2.1.2 Closed-loop (Indirect) Active System

This system is commonly used in those colder climates and instead of using the service water, heat-transfer liquids (usually a non-toxic propylene glycol-water antifreeze mixture) are used to circulate through the solar collectors. After leaving the solar collectors, the fluid will pass through a heat exchanger that placed inside the storage tanks and heat up the water that stored the tanks as depicted in Figure 2.3. The reason of using the antifreeze fluid is to prevent the piping of the system from freezing and increase the heat transfer rate from the collectors to the tanks.

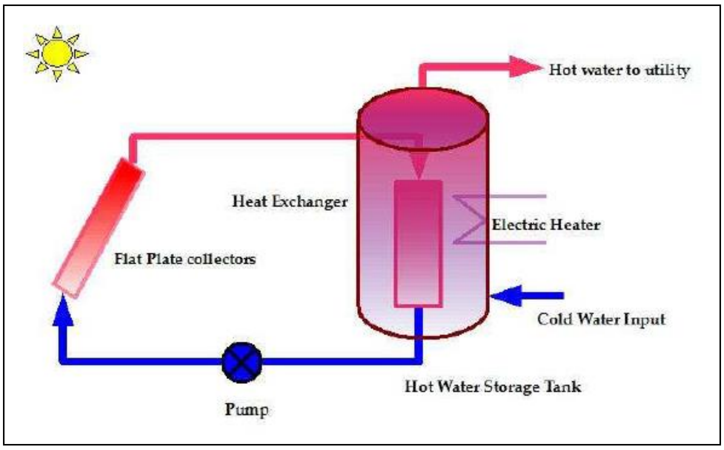

Figure 2.3: Closed-loop (Indirect) Active System (Johari et al., 2012)

2.2.2 Passive System

The passive system does not require any pumps or other electrical components for the circulation of water or a heat-transfer fluid between solar collectors and storage tanks. It circulates the water or heat-transfer fluid by natural convection where the storage tank is located at a higher level than the solar collectors (Shelke et al., 2014). The principle of natural convection is simple - the collector absorbs radiation from sun and heat up the water, the density of water will decrease as the temperature of water increases. As the density decreases, the water will become lighter and hence it will start flowing upward into the storage tank while the cold water at the bottom of the storage tank will run into the collector pipes and gets heated up there. Thermosyphon and integrated collector storage (ICS) systems are the most common types of passive systems.

2.2.2.1 Thermosyphon System

Thermosyphon system is simple and less maintenance is required due to the absence of electric pumps or controllers that are required in the active system. This system works based on the fact that cold water sinks and hot water rises. Water (cold) in this system is flowed from an overhead tank to bottom of solar collectors and when water is heated at the collectors, it will flows back into the storage tanks as illustrated in Figure 2.4. This process is a continuous cycle as long as there is solar radiation on the solar collectors. Besides that, the difference between collector temperature and ambient temperature will affect the efficiency of the collectors (Johari et al., 2012).

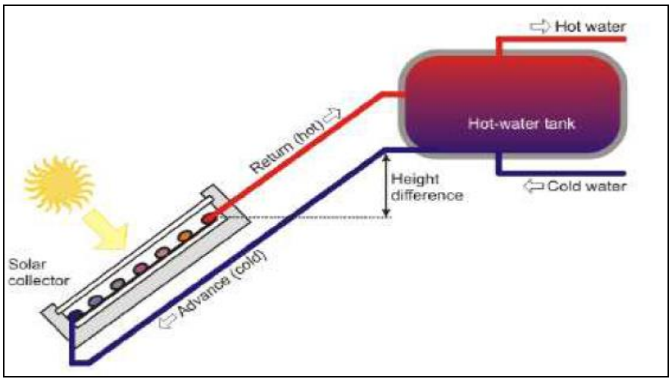

Figure 2.4: Thermosyphon System (Johari et al., 2012)

2.2.2.2 Integrated Collector Storage (ICS) System

It also known as batch system which is a simple passive system that used in warm climates. For this system, tank and collectors are combined into one unit and they are placed inside an insulated box with a glazed side facing the sun (Johari et. al, 2012). Figure 2.5 shows the integrated collector storage system. This system is simple effective and low cost as it does not need any pumps or moving parts. On the other hand, thermal protection of the storage tank is a weakness for this system as most of their surface is used for the absorption of solar radiation. As a result, the heat loss of the storage tank at night is relatively high so they only able to provide hot water during the day (Solar Energy – State of the art, 2001). Double glazing, transparent insulation materials and selective absorbing surface coatings are commonly used for the thermal protection of the ICS system.

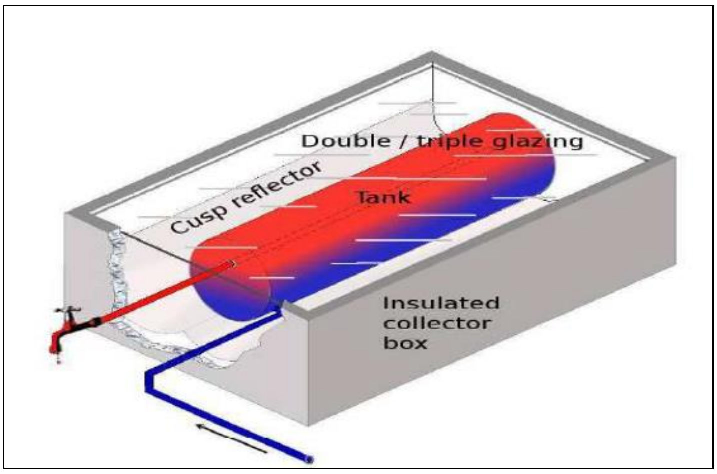

Figure 2.5: Integrated Collector Storage (ICS) System (Johari et al., 2012)

2.3 Solar Collector

A solar collector is designed to absorb solar irradiation and convert them into thermal energy. Solar collectors are available in many forms, sizes and shapes (Laughton, 2010). There are three common types of solar collectors such as flat plat collector, evacuated tube collector and also concentrating collector. For choosing a suitable collector, it mainly depends on the heating requirements and the environmental conditions (Johari et al., 2012).

2.3.1 Flat Plate Collectors

A flat plate collector is generally built by using flat sheet of absorber material and flat glazing. Normally, it is an insulated and weatherproof box that containing dark absorber plate with one or more transparent covers is shown in Figure 2.6. Inside the absorber, it contains pipes or passageways, which allows fluid to flow through and transport the heat away from the absorber. Absorber plate and pipes that used to construct this kind of collector are normally made of metal, such as copper, stainless steel or aluminium. On the other hand, the insulated enclosure box which is usually made of aluminium, plastic or even wood with glazing that made of glass or rigid and thin films of plastics (Laughton, 2010). The flat plate collector is designed to collect both direct and diffuse radiation. The design of the collector is simple and without any moving parts, so the manufacturing cost and maintenance requirements are minimal (Johari et al., 2012).

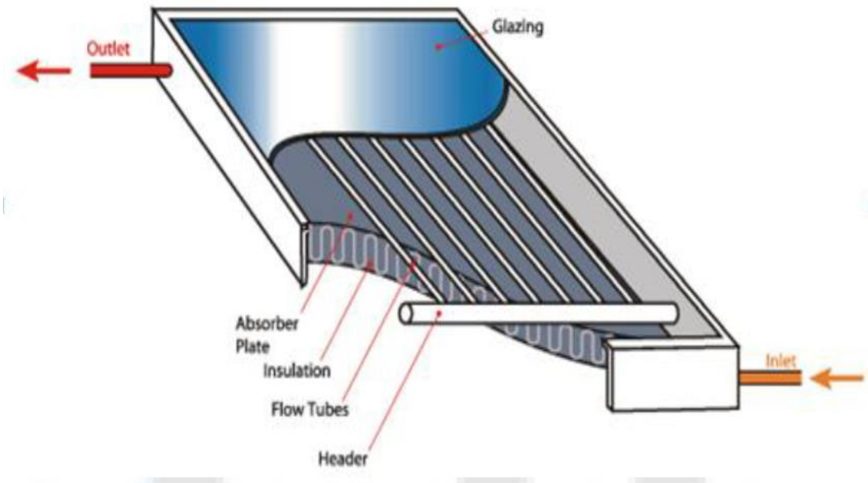

Figure 2.6: Flat Plate Collector (Shelke et al., 2014)

Besides that, there is usually a gap which about 2cm between the absorber and glazing. The function of this 2cm gap is to reduce the heat loss from the collector. If this gap is too narrow, radiation will be emitted back from absorber through the glazing and increases the heat loss. However, if it is too wide, unwanted warm air circulation in the system will be increase, and hence causing heat loss. A flat plate collector will operate at a temperature which around 40 to 80°C (100–180°F) under normal circumstances. Furthermore, the heat loss is directly proportional to the absorber temperature. As a result, the lower the absorber temperature, the smaller the amount of heat loss and hence the higher the efficiency of the collector. In order to further reducing the heat loss, some of the flat plate collectors are fitted in enclosures where the air is partially evacuated. The maximum stagnation temperature for a flat plate collector can be vary from 130°C to 200°C (260–400°F) in which any liquid in the collector will be evaporated into a gas. In addition, flat plate collectors need to be tilted at least 15 degrees from the horizontal to facilitate drainage of rain water and air removal from the collector glazing and absorber respectively (Laughton, 2010).

2.3.1.1 Efficiency of a Flat Plate Collector

The power output of a collector, P_u can be computed by using the following formula:

$$P_u = \eta_c A_p G \tag{2.1}$$

where η_c is the efficiency of the collector, A_p is the area which exposed to irradiance and G is the solar irradiance.

The collector's efficiency, η_c can be further divided into two different stages which are the capture efficiency (η_{sp}) and the transfer efficiency (η_{pf}):

$$\eta_c = \eta_{sp} \eta_{pf} \tag{2.2}$$

where the capture efficiency is

$$\eta_{sp} = \tau_{cov} \alpha_p - U_L(T_p - T_a)/G \tag{2.3}$$

which shows that as the plate temperature increases, the losses will increase until η_{sp} reduces to zero at the "equilibrium" temperature $T_p^{(m)}$, which also known as the stagnation temperature. As the plate temperature T_p of an operating collector is not usually known, so it is more suitable to relate the useful energy gain to the mean fluid temperature $\bar{T}_f$. Hence:

$$\eta_c = P_u /(AG) = \eta_{pf} \tau_{cov} \alpha_p - \eta_{pf} U_L(\bar{T}_f - T_a)/G \tag{2.4}$$

where τ_{cov} is the transmittance of transparent cover, α_p is the fraction of flux being absorbed, U_L is the coefficient of overall heat loss and T_a is the ambient temperature. For a well-designed collector, the difference between the temperature of the plate and the transfer fluid is small and the value of η_{pf} is approximately equal to one. Typically, η_{pf} is equals to 0.85 and is practically independent of the operating conditions, and, since pipes and storage tanks should be well insulated, so $\bar{T}_f \approx T_p$. Hence the U_L in Eq. 2.4 is numerically almost the same as that in Eq. 2.3. As a result, the capture efficiency η_{sp} and the collector efficiency η_c would change linearly with temperature if $U_L = 1/(A_P R_L)$ which is a constant in (2.3) and (2.4), but in fact the radioactive resistance decreases significantly as T_p increases. Hence, a graph of η_c against operating temperature is plotted, as shown in Figure 2.7.

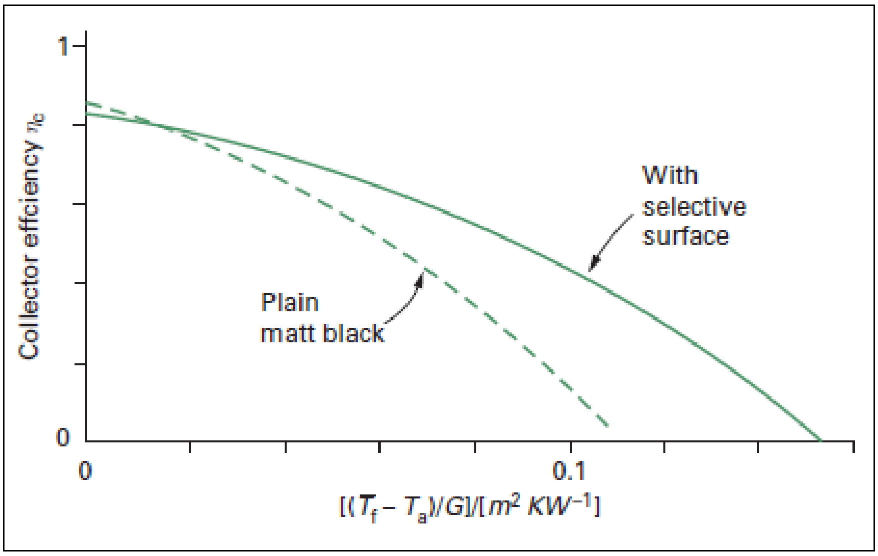

Figure 2.7: Graph of η_c against Operating Temperature (Twidell and Weir, 2015)

2.3.2 Evacuated Tube Collectors

An Evacuated Tube Collector is made up of rows of parallel, transparent glass tubes which mounted in rows and inserted into a manifold box as illustrated in Figure 2.8. Each tube consists of an absorber in it, which usually a strip of metal or glass that covered with a selective coating that absorbs solar radiation well but at the same time inhibits radiative heat loss. Normally, the air from the space between the tubes is removed or evacuated in order to create a vacuum which acts as insulation and reduces heat loss. The evacuated tube collector is most suitable for the extremely cold ambient temperature areas or in the areas where consistently low-light (Johari et al., 2012). This is because of the absorber in the evacuated tube collector is located in a vacuum space in which the effect of external ambient temperature on the performance will be minimal. In other words, this means that an evacuated tube collector will mostly outperform a flat plate collector on a cold sunny day (Laughton, 2010). Besides from domestic usage, it also can be used in industrial applications in which high water temperature or steam need to be generated (Johari et al., 2012).

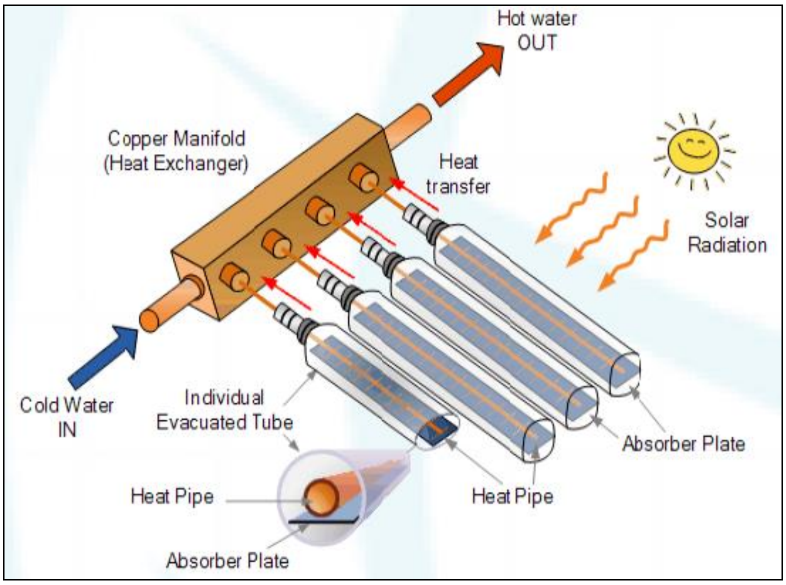

Figure 2.8: Evacuated Tube Collector (Shelke et al., 2014)

2.3.3 Concentrating Collectors

The concentrating collector is a solar collector that used reflective surfaces to concentrate the sun's ray onto an absorber which also known as a receiver. Inside the receiver, it allows heat transfer fluid to flow through and transfer the heat away from it. The temperature of this collector can reach much higher compared to the flat plate collectors and evacuated tube collectors, but they only able to do so when direct sunlight is available. Furthermore, the concentrators can only focus direct solar radiation, therefore their performance on hazy or cloudy days will be relatively low (Johari et al., 2012).

For concentrating collectors, they can be distinguished into two categories which are stationary collectors and sun tracking collectors. One of the examples of stationary concentrating collectors is compound parabolic concentrator (CPC). CPC collectors are non-imaging collectors that having the ability to accept incoming solar radiation over a wide-ranging angles and reflect most of the radiation to the absorber which located at the bottom of the collector. Winston's CPC which is the most common type of CPC collectors is shown in Figure 2.9 (Shulka et al., 2013). On the other hand, CPC is hard to fabricate and the imperfection of its symmetrical design may occurred during the manufacturing process, and hence reduce its effectiveness. Figure 2.10 shows the imperfection of CPC collector in which the surface of the collector full with waviness.

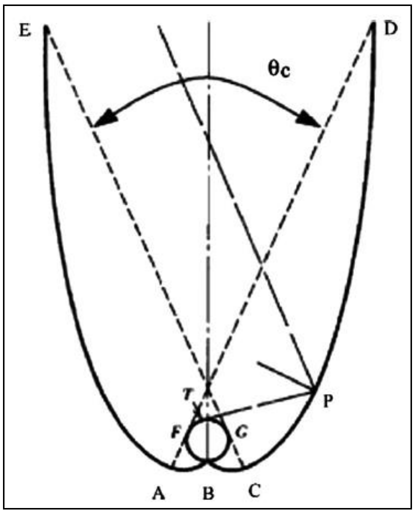

Figure 2.9: Schematic diagram of a CPC collector (Shulka et al., 2013)

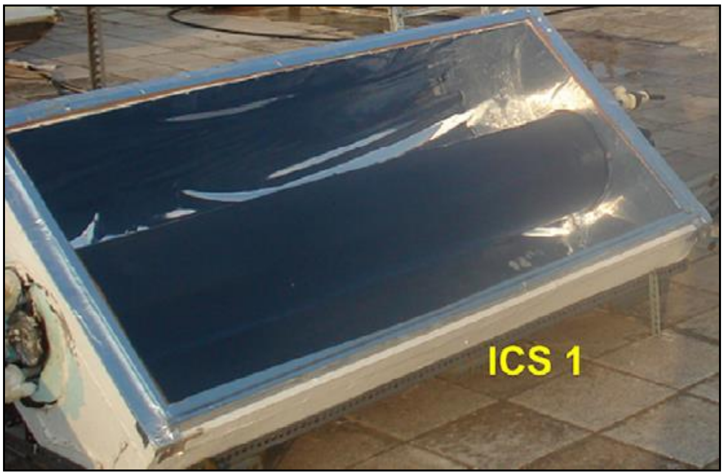

Figure 2.10: Imperfection of CPC Collector (Souliotis et al., 2013)

On the other hand, parabolic trough collectors are one of the sun tracking collectors. It can efficiently produce heat at temperature within 50-400°C. It is made by a sheet of reflective material which is bending into parabolic shape and a heat pipe which normally paints in black that covered with a glass tube to minimize heat loss and located along the focal line of the receiver as depicted in Figure 2.11. When the parabola is directly faced towards the sun, parallel rays that fall on the collector are then reflected onto the receiver tube. In addition, a single axis tracking of the sun is sufficient for it and hence result in long collector modules (Kalogirou, 2004).

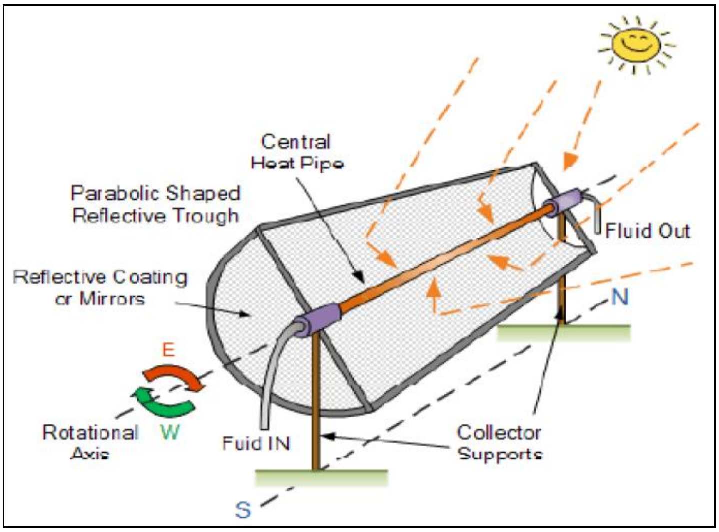

Figure 2.11: Concentrating Collector (Shelke et al., 2014)

CHAPTER 3

METHODOLOGY

3.1 Overview

This chapter is about the methodology of the study. Figure 3.1 illustrates the flow of the study. First, design the optical geometry of multiple linear facets ICSSWH with trigonometry approach. Next, the optical design is validated by using ray tracing software. Subsequently, the mechanical structure of the multiple linear facets ICSSWH is designed and constructed. Then, the performance of the ICSSWH is evaluated.

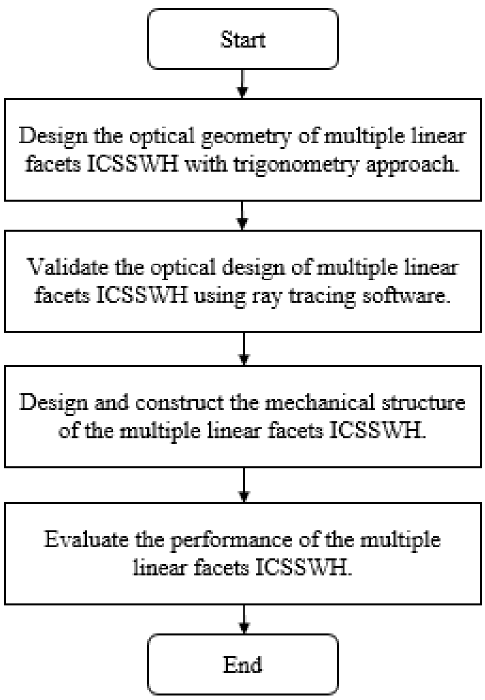

Figure 3.1: Flowchart of Methodology

3.2 Optical Design of Multiple Linear Facets ICSSWH

To create the optical design of the multiple linear facets ICSSWH, there are some steps that must be followed in order to determine the angle and length for different mirrors. Lastly, SolidWorks was used to draw out the final design of the multiple linear facets ICSSWH.

Step 1: Determine the length of the base mirror.

A circle and two straight lines were draw as shown in Figure 3.2. The circle represents the tank of the ICSSWH while the line under the tank represents the base mirror of the ICSSWH and another line represents the ray that enter the ICSSWH with 90° which means the sun is directly on top of the tank. With this, the length of the base mirror was obtained as its length is same as the radius of the tank (ℓ_{base} = r).

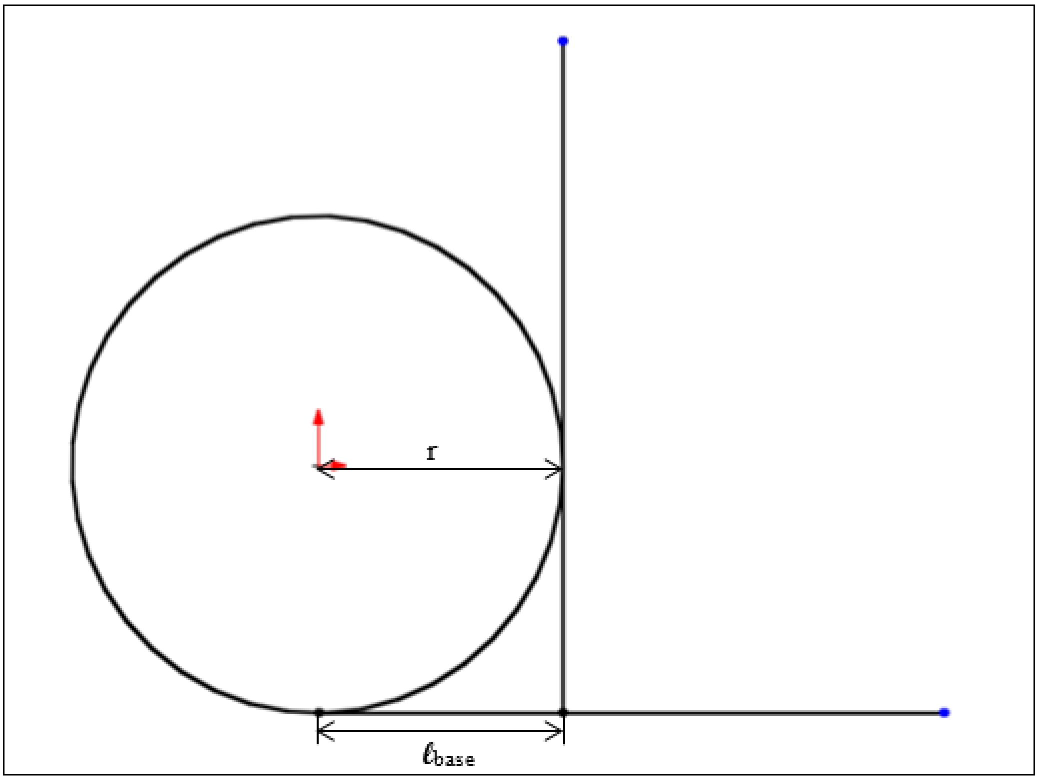

Figure 3.2: Determine the Length of the Base Mirror

Step 2: Set an Angle for First Slanted Mirror.

At the intersection point of the 90° ray and the base mirror, a slanted line which represents the mirror has an angle of 45° from the base mirror was draw as shown in Figure 3.3. 45° angle was selected is because when 90° ray falls on the mirror, the ray will be reflected perpendicularly to the bottom most surface of the tank and hence the maximum ray energy will fall on the surface of the tank.

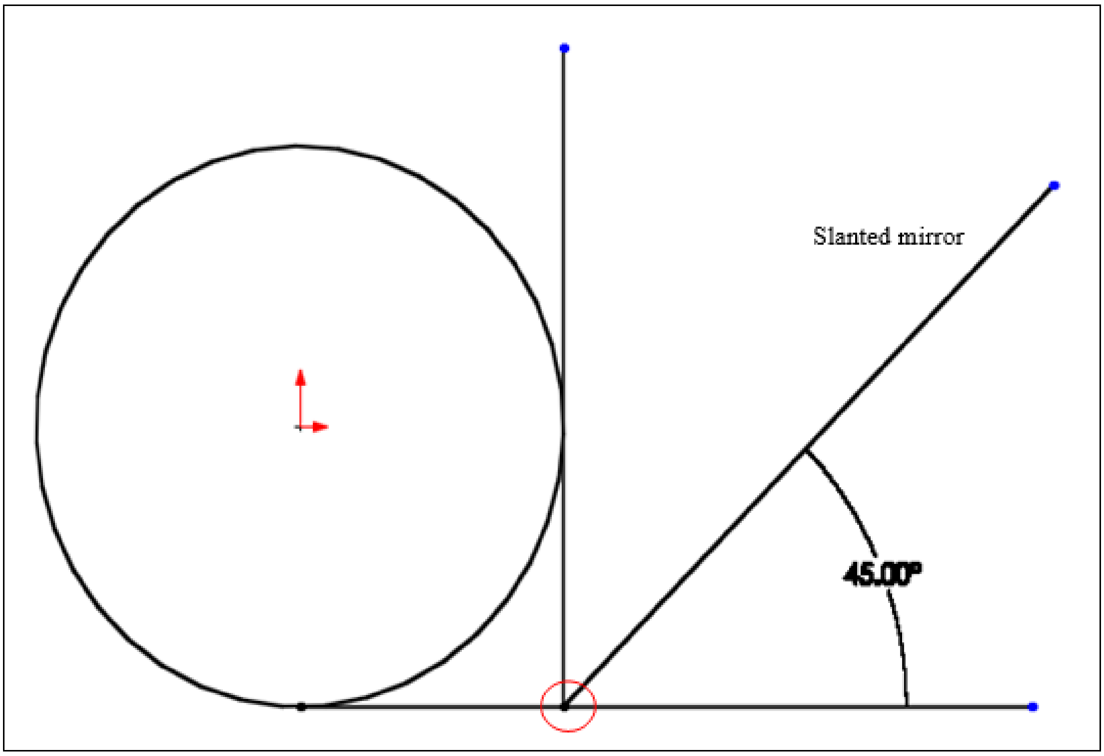

Figure 3.3: A Slanted Line with 45° Angle was Draw

Step 3: Determine the Length of First Slanted Mirror.

For our study, the multiple facets ICSSWH will be setup at Kampar, Malaysia which has the coordinate of 4.3085°N, 101,1537E. Because of the design was set to have east-west configuration and the maximum sun declination angle is 23.45°, hence the half acceptance angle of the ICSSWH should be 28° (rounding up) in which it summed up the latitude of Kampar and the maximum sun declination angle. Therefore, the incident ray with 28° angle must be reflected by the mirror and its reflected ray must be tangent to the surface of the tank as illustrated in Figure 3.4 so that all the incident ray with the range of 0° to 28° angle able to be reflected onto the tank.

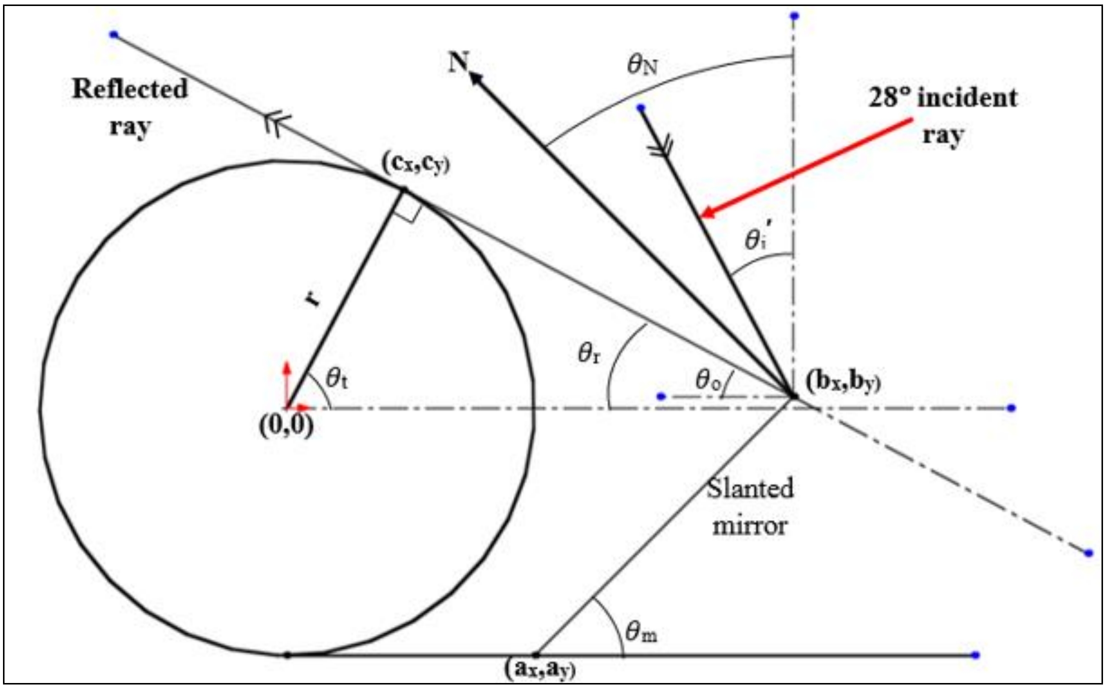

Figure 3.4: Determine the Reflected Ray

Referring to Fig. 3.4, the length of the slanted mirror can be written as

$$\ell_m = \sqrt{(b_x - a_x)^2 + (b_y - a_y)^2} \tag{3.1}$$

where (a_x,a_y) and (b_x,b_y) are the end points of base mirror and slanted mirror respectively. Since the length of the base mirror equals to the radius of the tank, so $(a_x,a_y) = (+r,-r)$ and the midpoint of the tank is (0,0) in which r is the radius of the tank. For (b_x,b_y), the equations of two straight lines which are the slanted mirror and reflected ray are needed.

The line equation for the slanted mirror is written as

$$y = m_m x + c_m \tag{3.2}$$

where m_m is the gradient of the slanted mirror in which it can be calculated by using

$$m_m = \tan \theta_m \tag{3.3}$$

and for the c_m, it represents the y-intercept of the line and it can be obtained by substituting (a_x,a_y) into Eq. 3.2.

On the other hand, the line equation for the reflected ray is written as

$$y = m_r x + c_r \tag{3.4}$$

where m_r is the gradient of the reflected ray and it is calculated as

$$m_r = \tan \theta_r \tag{3.5}$$

in which $\theta_r = \theta_o = \theta_i$ and the c_r is the y-intercept of the line. c_r can be obtained by substituting the coordinate of the intersection points of tank surface and reflected ray which is (c_x,c_y) into the Eq. 3.4.

In order to obtain the value of (c_x,c_y), the equations below were used

$$c_x = r \cos \theta_t \tag{3.6}$$

$$c_y = r \sin \theta_t \tag{3.7}$$

where r is the radius of the tank and the θ_t is the angle between the center line of the tank and the tank's radius which perpendicular to the reflected ray. θ_t can be calculated by using trigonometry as

$$\theta_t = 180 - 90 - \theta_r \tag{3.8}$$

Hence, by solving Eqs. 3.2 and 3.4 simultaneously, the value of x and y can be obtained and they represent b_x and b_y respectively.

Step 4: Determine the Angle for Next Mirror.

A 90˚ straight line which represents the incident ray was draw at the end of the first slanted mirror. Next, a line which represents its reflected ray was draw from the end of the first slanted mirror and it was tangent to the bottom of the tank's surface as shown in the Figure 3.5.

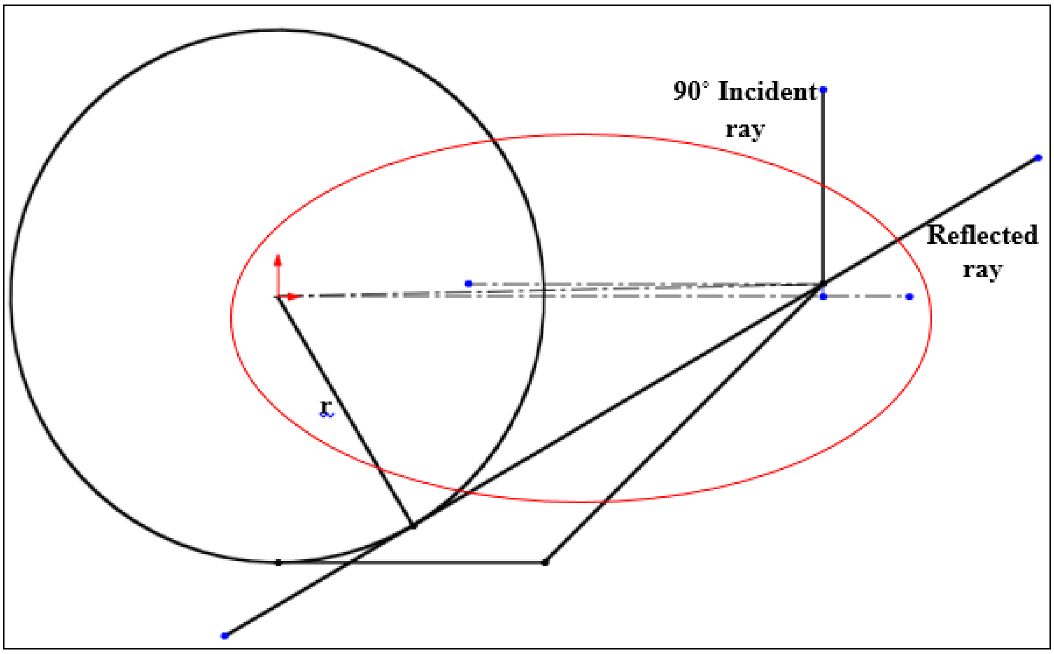

Figure 3.5: Determine the Angle for Next Mirror

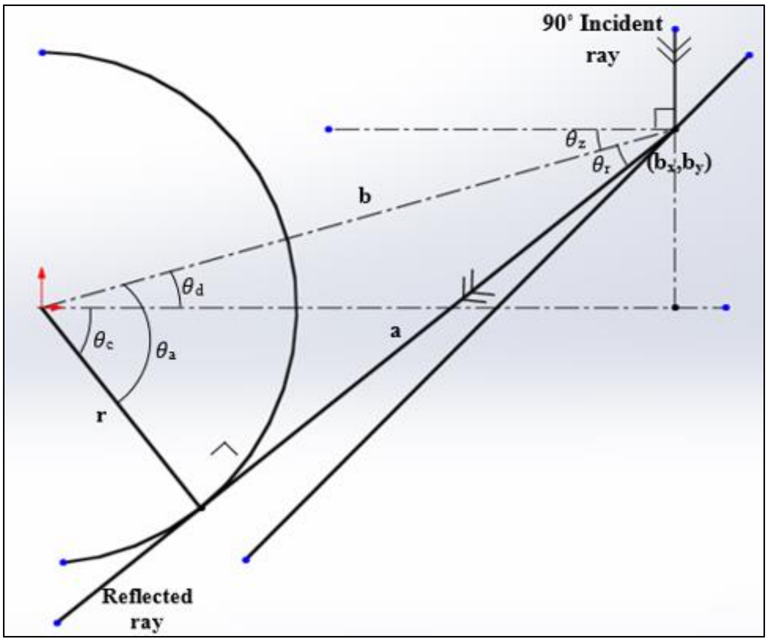

Figure 3.6: Clearer View of the Circled Part in Figure 3.4

Referring to Figs. 3.5 and 3.6, the angle of the next mirror from the base mirror is written as

$$\theta_{m(new)} = \frac{\theta_T}{2} \tag{3.9}$$

where θ_T is the angle of reflection of the 90° angle incident ray from the new mirror.

For the θ_T, it can be calculated as

$$\theta_T = 90 + \theta_r + \theta_z \tag{3.10}$$

where θ_r is the angle between the reflected ray and a straight line which from the midpoint of the tank to the end point of first slanted mirror. θ_r is calculated as

$$\theta_r = \tan^{-1}\frac{r}{a} \tag{3.11}$$

in which r is the radius of the tank and *a* is the distance from the intersection point of reflected ray and tank surface to the end point of first slanted mirror. *a* can be obtained as

$$a = \sqrt{b^2 - r^2} \tag{3.12}$$

in which *b* is the distance from the midpoint of the tank to the end point of first slanted mirror and it can be calculated by substituting (0,0) and (b_x,b_y) into the formula below

$$Distance = \sqrt{(x_2 - x_1)^2 + (y_2 - y_1)^2} \tag{3.13}$$

and for θ_z, it is the depression angle from the end point of first slanted mirror to the midpoint of the tank. θ_d need to be obtained in order to find θ_z since $\theta_z = \theta_d$. θ_d is calculated as

$$\theta_d = \tan^{-1} \frac{b_y}{b_x} \tag{3.14}$$

Step 5: Repeat Steps 3 and 4 to Find Other Mirrors.

The concepts of determining the length and angle for the mirror in steps 3 and 4 were repeated to obtain second mirror and so on. Hence, one side of the collector for multiple linear facets ICSSWH was formed (Figure 3.7) and the dimension of it can be used to create the other side of the collector.

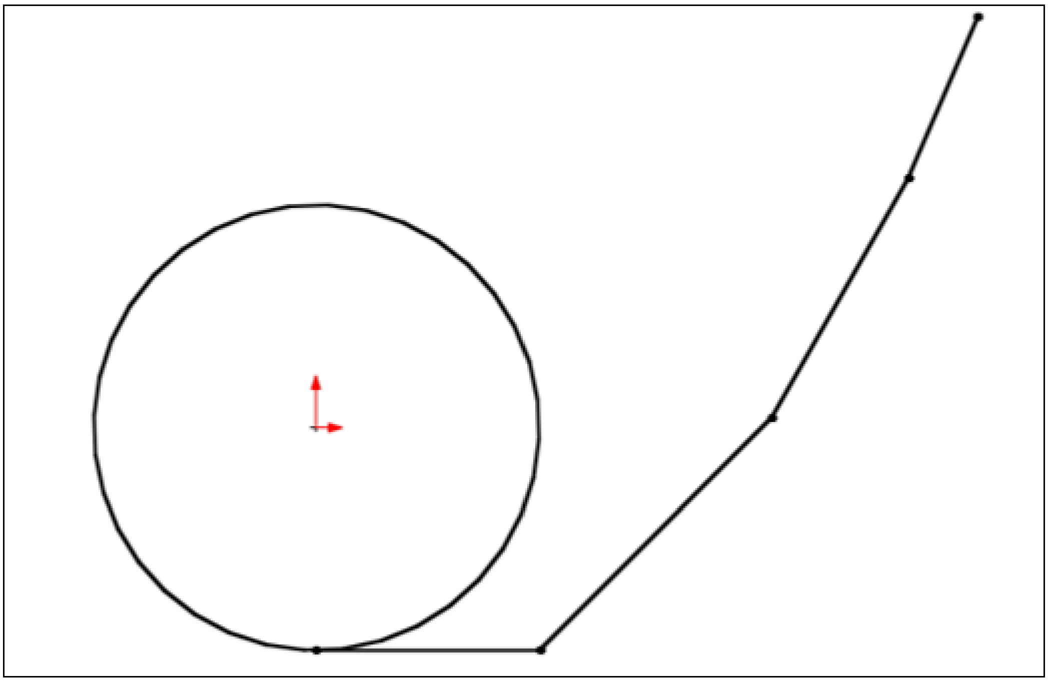

Figure 3.7: One Side of the Collector

Step 6: Using SolidWorks to Create the 2D and 3D Models for the Collector.

Lastly, SolidWorks was used to create the 2D (Figure 3.8) and 3D (Figure 3.9) models of the multiple linear facets ICSSWH based on the dimension that obtained from the previous steps. The dimension and angle for different mirrors for one side of the collector is tabulated in Table 3.1.

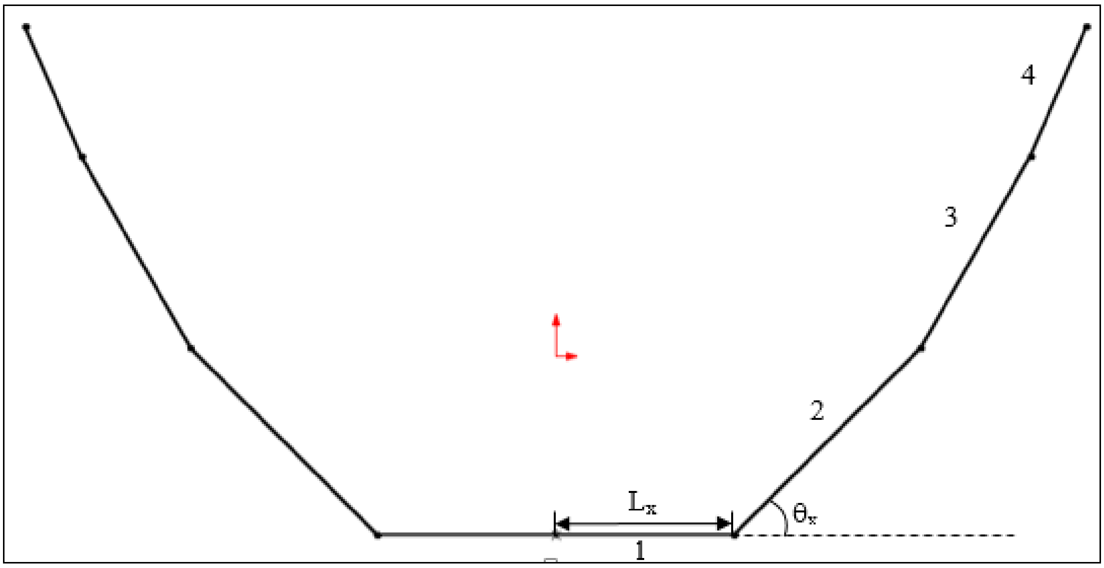

Figure 3.8: Complete 2D model of the Collector

Table 3.1: The Length and Angle for Different Mirrors for One Side of the Collector

X	Length of the mirror, L_x (mm)	Angle of the mirror, θ_x (°)
1	83.00	0
2	122.68	45.0
3	102.88	60.3
4	65.28	66.6

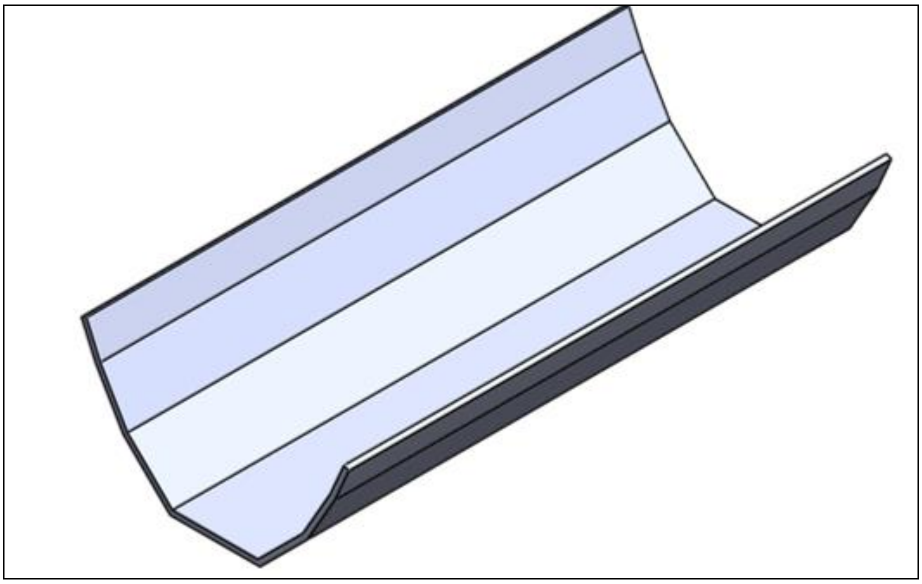

Figure 3.9: 3D Model of the Optical Design

3.3 Ray Tracing for the Optical Design of Multiple Linear Facets ICSSWH.

The file of the complete optical design was then saved as Initial Graphics Exchange Specification (IGES) file which allows the user using the 3D design in different Computer Aided Design (CAD) software. The IGES file was the imported to TracePro, a ray tracing software to test and validate the optical design of multiple linear facets ICSSWH.

In TracePro, a water tank with a radius of 83mm was added to the middle of the optical design with a 5mm gap above the base mirror. The graphic user interface (GUI) of adding the water tank was shown in Figure 3.10. Besides that, the property of the surface of the water tank and the facet mirrors of the optical design were changes to “perfect absorber” and “mirror” respectively. Figures 3.11 and 3.12 show the GUI of the updated property for water tank and facet mirrors respectively.

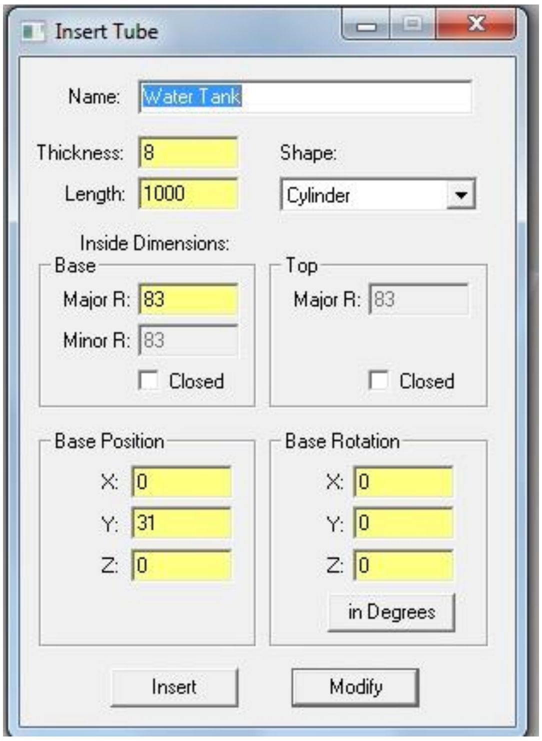

Figure 3.10: GUI of Adding Water Tank

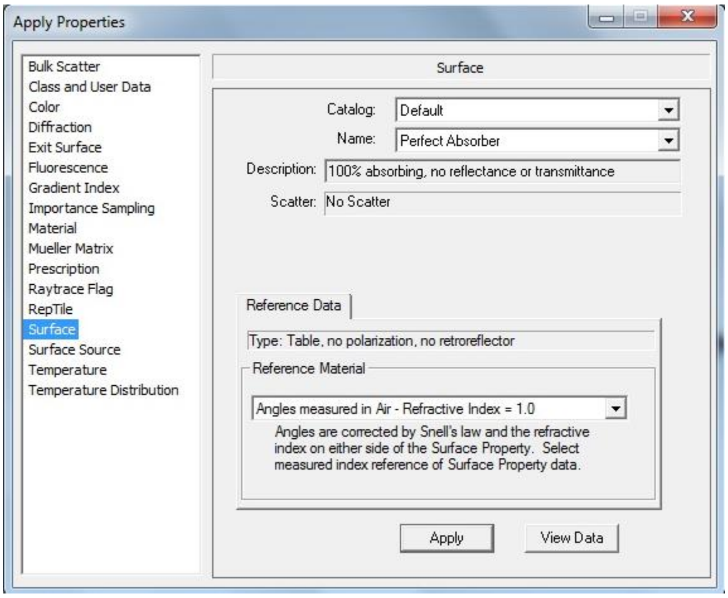

Figure 3.11: GUI of Updating the Property of Water Tank

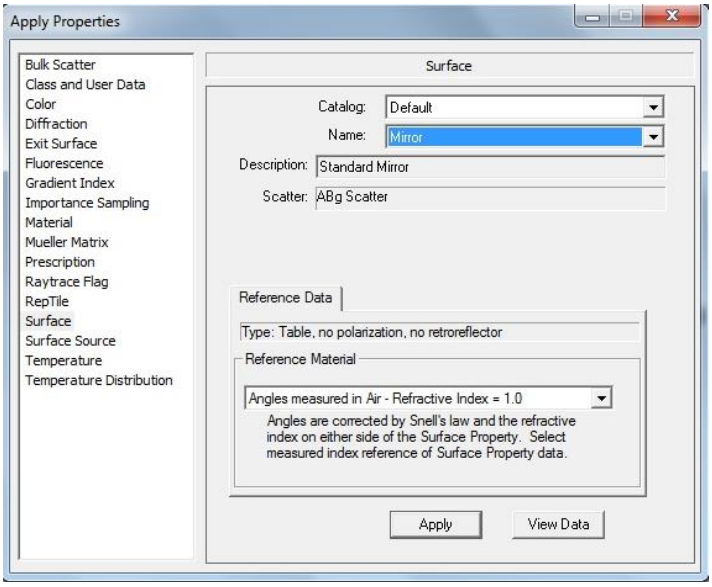

Figure 3.12: GUI of Updating the Property of Facets Mirrors

Furthermore, the grid source which represents the sun in the ray tracing program is defined as shown in Figure 3.13. The Y half-height and X half-width of grid boundary are set to 300 and 5 respectively in order to fully cover the optical design. The irradiance value is set to 1000W/m^2. The origin is set by adjusting the values of X, Y and Z to ensure the grid source is directly on top of the optical design. Next, the normal vector is used to adjust the angle of the grid source by changing the values of X, Y and Z while the Y value must be in negative to ensure the rays shot downwards to the optical design. The X-up vector is set to 1 as normal ground.

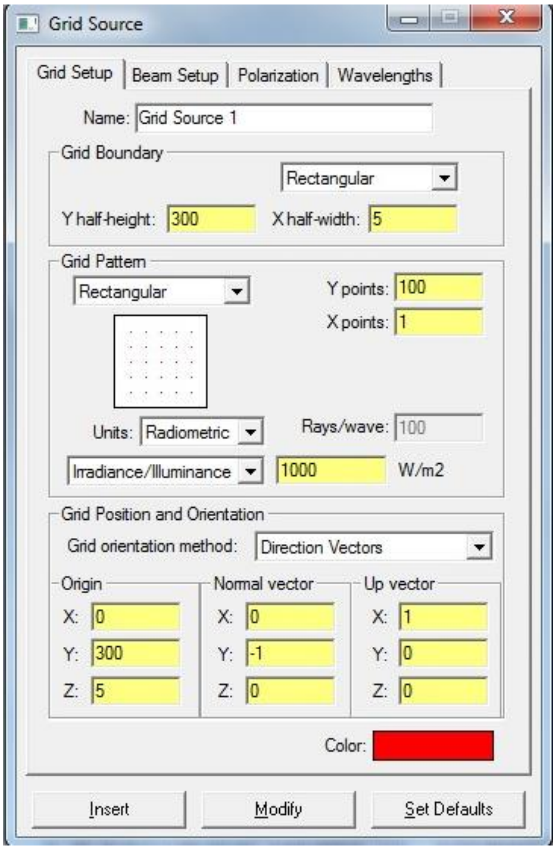

Figure 3.13: GUI of Grid Source Parameters Setting

Lastly, different incident angles are tested to validate and ensure the rays enter the multiple linear facets ICSSWH design completely. The mentioned incident angles from y-axis are 0˚, 5˚, 10˚, 15˚, 20˚, 25˚, and 28˚. The ray tracing of the optical design at different incident angles respectively are shown in Figure 3.14.

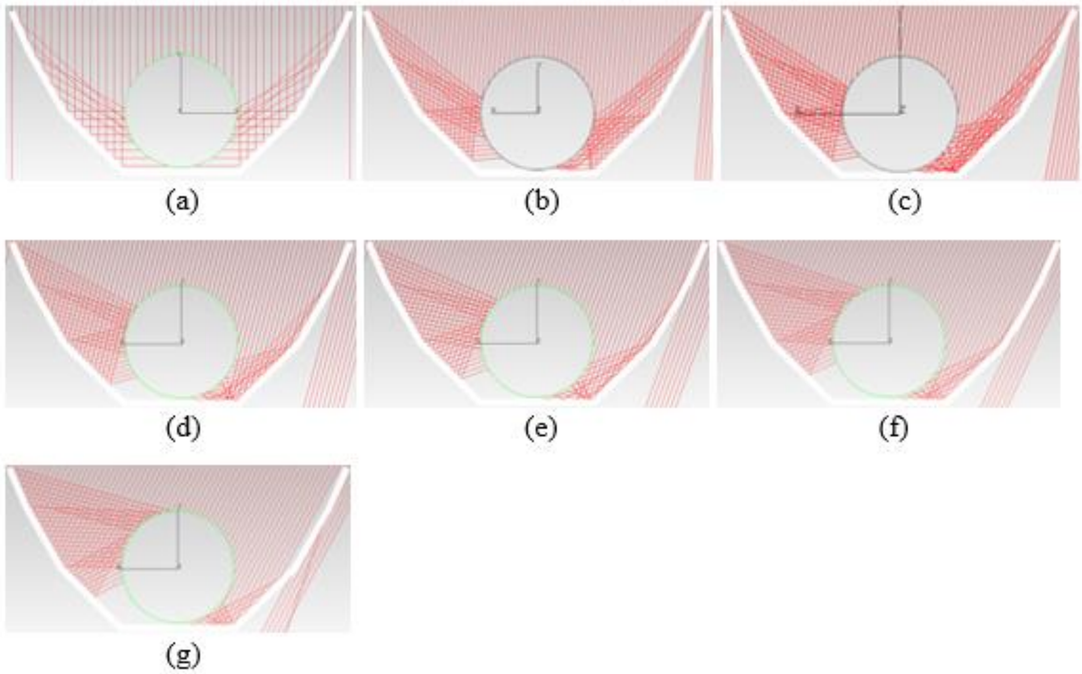

Figure 3.14: Ray Tracing of the Optical Design of Multiple Linear Facets ICSSWH at Different Incident Angles. (a) 0°, (b) 5°, (c) 10°, (d) 15°, (e) 20°, (f) 25°, and (g) 28°

3.4 Design and Construct the Mechanical Structure of Multiple Linear Facets ICSSWH.

SolidWorks is used for designing the 3D model of the multiple linear facets ICSSWH. The complete design of multiple linear facets ICSSWH contains wooden box, mirrors, water tank with piping system, acrylic boards as well as clear float glass. All of the parts were designed individually and assembly together to form the complete multiple linear facets ICSSWH. The technical drawing of the whole assembly and the complete 3D model of multiple linear facets ICSSWH are shown in Figures 3.15 and 3.16 respectively.

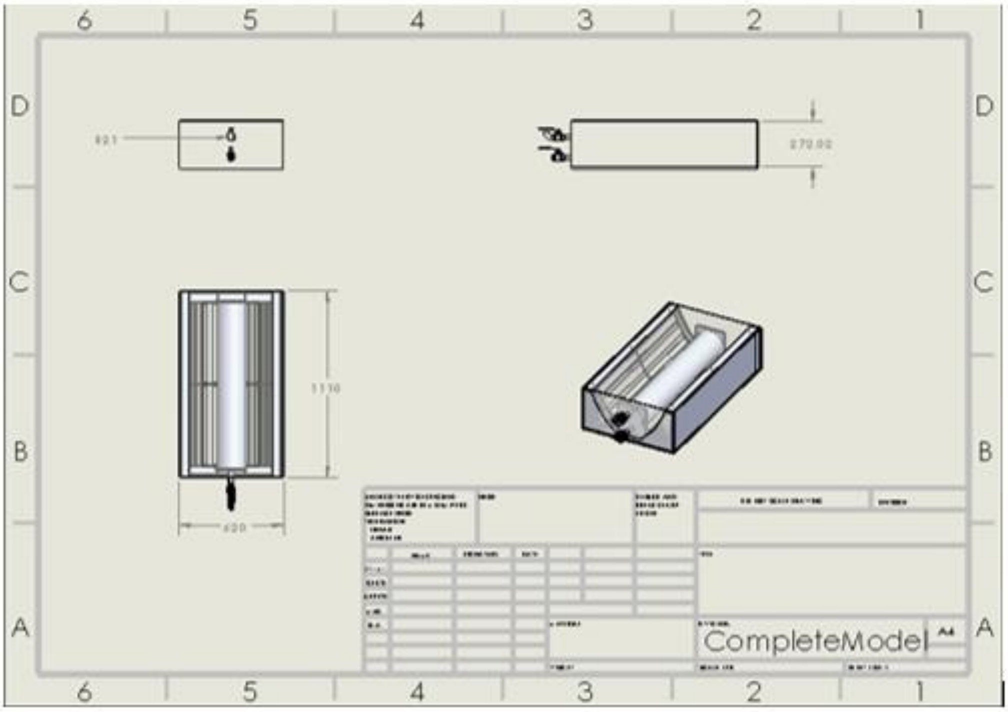

Figure 3.15: Technical Drawing of Multiple Linear Facets ICSSWH

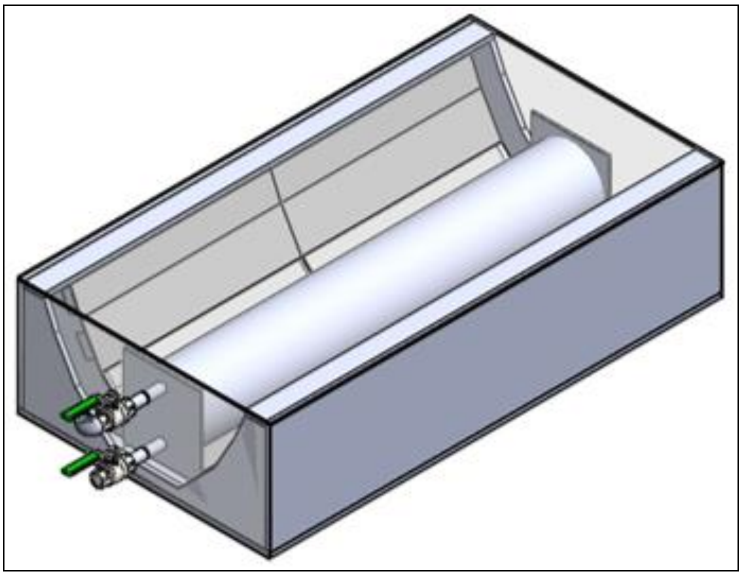

Figure 3.16: 3D Model of Multiple Linear Facets ICSSWH

For the prototype of the multiple linear facets ICSSWH, it was manufactured in Universiti Tunku Abdul Rahman, Kampar. The specifications of the different components of the multiple linear facets ICSSWH system and the techniques to construct the components are explained in detailed in the following section.

3.4.1 Wooden Box

The wooden box is made from two major parts: supportive frame for mirrors and wooden sheets that used to cover the frame. The supportive frame was created based on the profile of the optical design of multiple linear facets ICSSWH that has been validated by the ray tracing software. The profile of the optical design was drawn on the plywood sheets and cut made (Figure 3.17). Five such strips were made and three of it were undergo an extra process in which notches were cut as shown in Figure 3.18. Wooden strips were slotted into these notches in order to stabilize the frame and create a space for mirrors to fix on it (Figure 3.19). The other two pieces of the strips were used to cover the front and back of the frame, while three pieces of plywood sheets were cut based on the dimension that needed to cover the sides and bottom of the frame. For the sides, it needed two rectangular plywood sheets with a dimension of 272mm (width) × 1104mm (length) × 12mm (thickness) each. On the other hand, the bottom cover required a rectangular plywood sheet with a dimension of 617mm (width) × 1104mm (length) × 12mm (thickness). In addition, shellac was applied onto each of the plywood sheets and wooden strips so that the wooden frame is water-resistant and hence able to last for a longer period. Hence, the wooden box is completed.

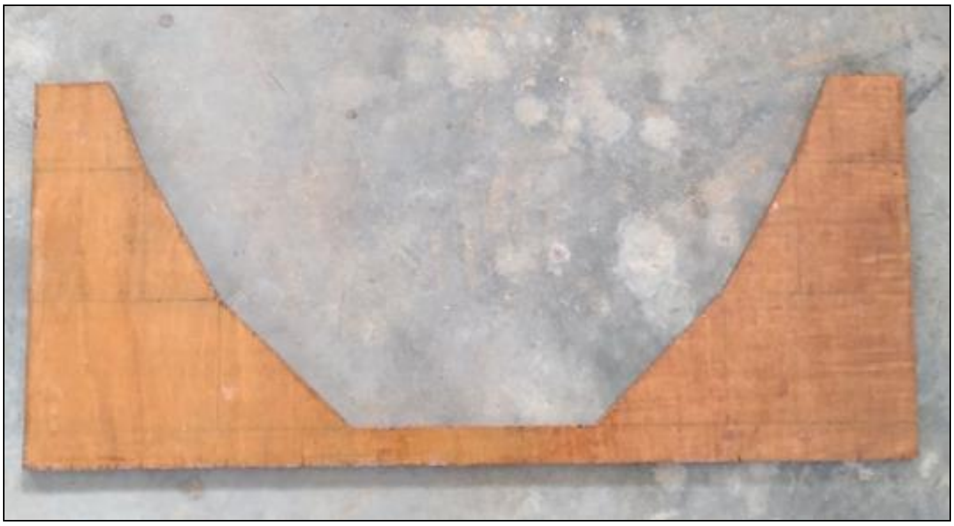

Figure 3.17: The Profile of the Supportive Frame

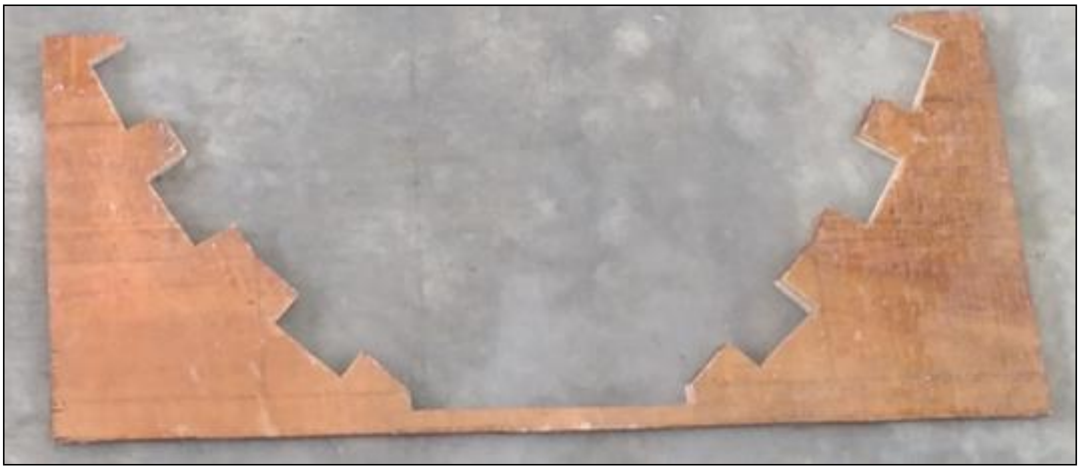

Figure 3.18: Supportive Frame with Notches

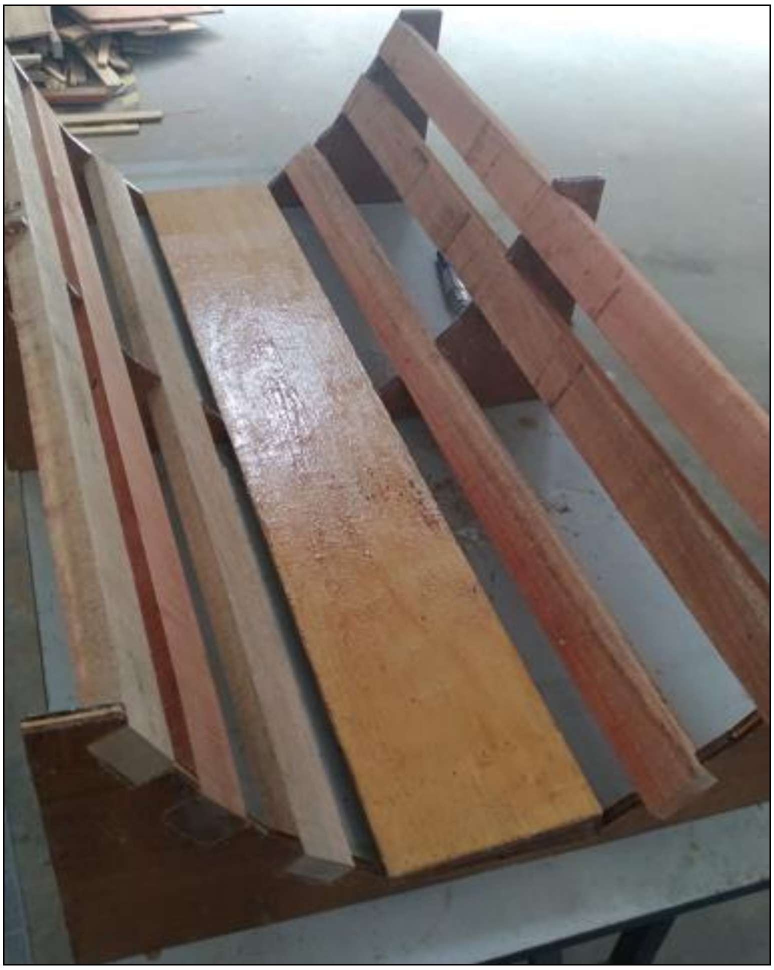

Figure 3.19: Complete Supporting Frame for Mirrors

3.4.2 Reflector

For this project, mirror with low iron silver coating was used to act as the reflector for this ICSSWH system. Mirror with 3mm thickness and a reflectivity of 0.96 was used. Different lengths of mirrors were cut according to the optical design and attached to the wooden frame by using adhesive (Figure 3.20).

Figure 3.20: Mirrors were attached to the Supportive Frame

3.4.3 Water Tank

The water tank was made by a 166mm diameter galvanized iron pipe which is 1m long and two pieces of metal plates with a dimension of 200mm (length) x 190mm (width) x 5mm (thickness) each. Welding process was used to join the pipe and metal plates together to form a metal tank. Two 22cm holes were drilled on one of the metal plates for the piping system in order to add or retrieve water from the tank. After that, the whole tank was painted black as to maximize its heat absorptivity. The tank was placed in the middle of the wooden box (Figure 3.21) so that all the reflected rays fall on the surface of the tank.

Figure 3.21: Water Tank with Piping System

3.4.4 Insulation & Glazing

Polyfoam was added to the side and bottom between the supportive frame and the covers to act as insulating material which helps to improve the heat retaining capability of the ICSSWH. In addition, the air gap inside the wood box also an additional thermal resistance for the ICSSWH. Besides that, two acrylic boards (front & back) and a glass cover (top) were used to cover the wood frame (Figure 3.22). They act as the glazing for the system which can protect the tank from the environment as well as reduce radiative heat losses.

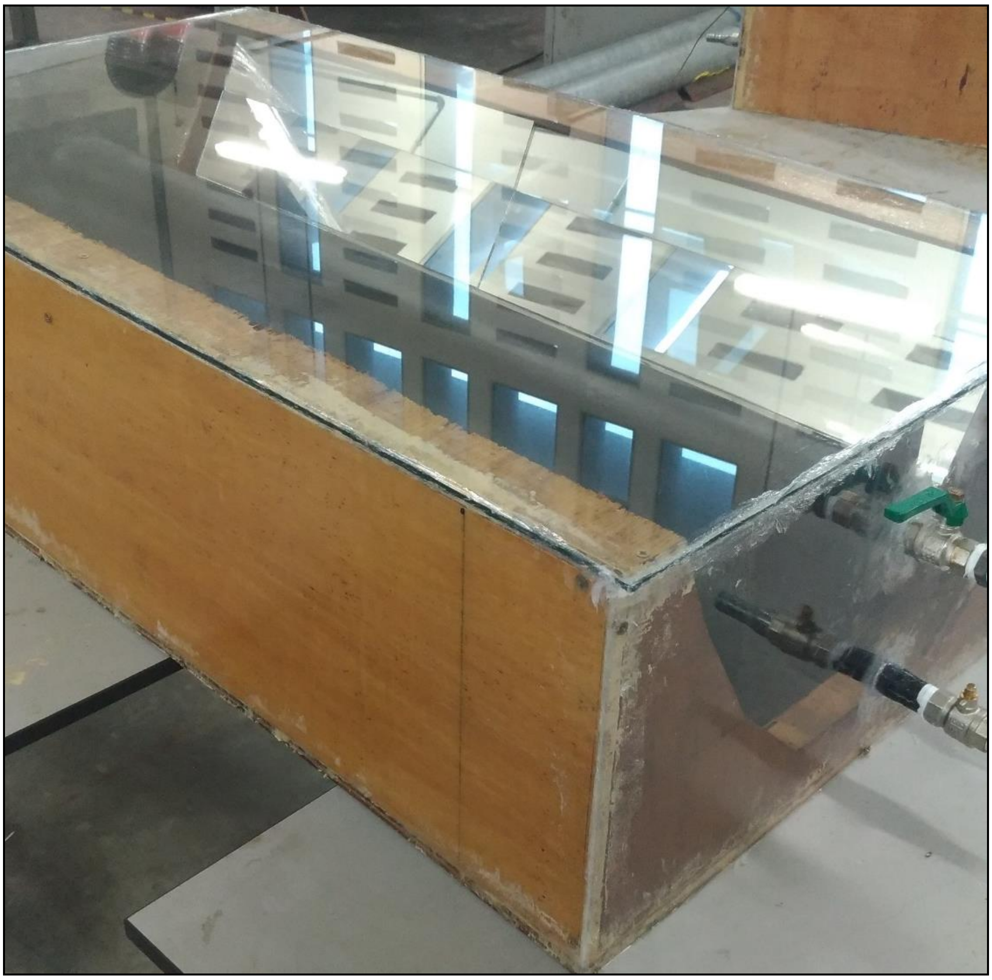

Figure 3.22: Wooden Box with Glass and Acrylic Boards

3.5 Evaluation on the Performance of the Multiple Linear Facets ICSSWH.

The performance of the multiple linear facets ICSSWH is evaluated by measuring the temperatures of the water, tank surface, and ambient. In order to measure the temperatures, thermocouples and thermocouple reader are used. Besides that, the temperature data are recorded every 5 minutes. In addition, pyranometer is used to obtain the value of global horizontal irradiance (GHI) and the time interval to record GHI data is 1 minute. Fig. 3.23 shows the tank surface, water and ambient temperature data collection.

Figure 3.23: Tank surface, Water and Ambient Temperatures Data Collection

CHAPTER 4

RESULTS AND DISCUSSION

4.1 System Performance of Multiple Linear Facets Integrated Collector Storage Solar Water Heater

The thermal performance of the prototype was evaluated and data collection was carried out in four different days. For data collection, tank surface temperature, water temperature in the storage tank, ambient temperature as well as global solar irradiance in the function of local clock time were measured and recorded. The measurement results for four different days which are 25th Jan 2018, 10th Feb 2018, 2nd Mar 2018 and 17th Mar 2018 are shown in Fig. 4.1, 4.2, 4.3 and 4.4 respectively

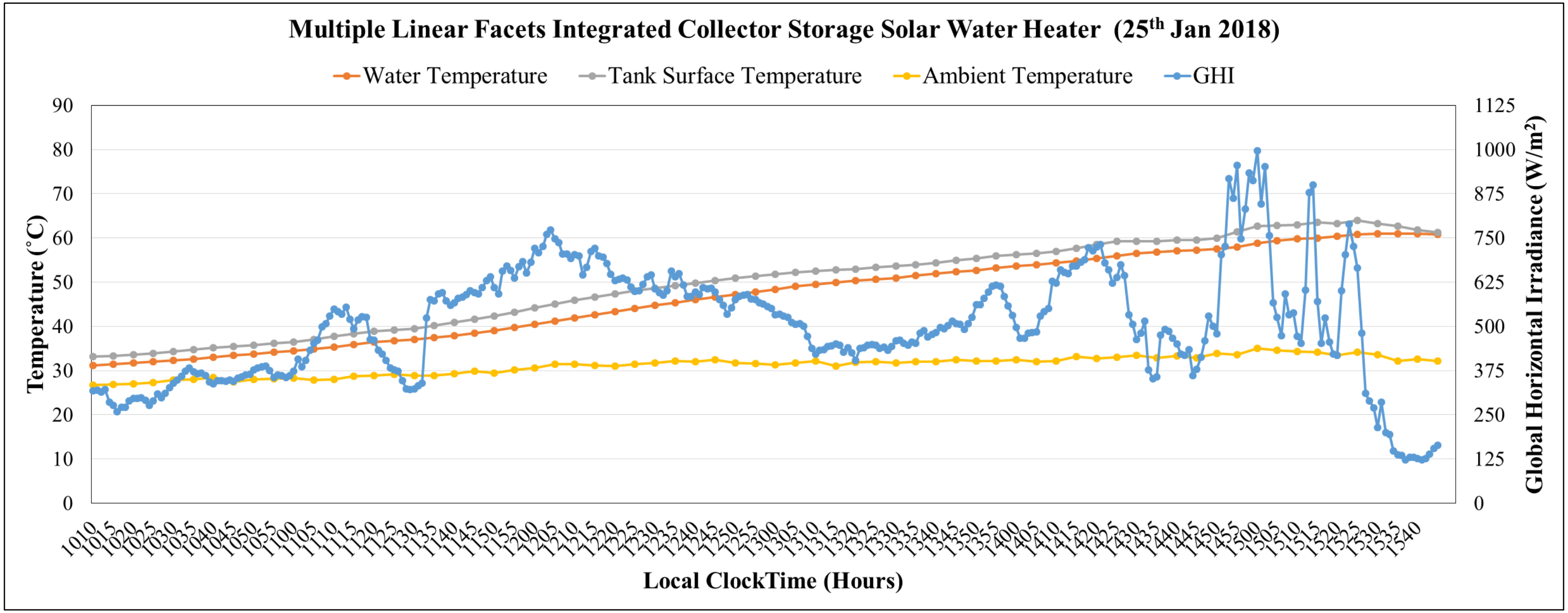

Figure 4.1: Measurement Results of Tank Surface Temperature, Water Temperature in the Storage Tank, Ambient Temperature and Global Solar Irradiance versus Local Clock Time on 25th Jan 2018

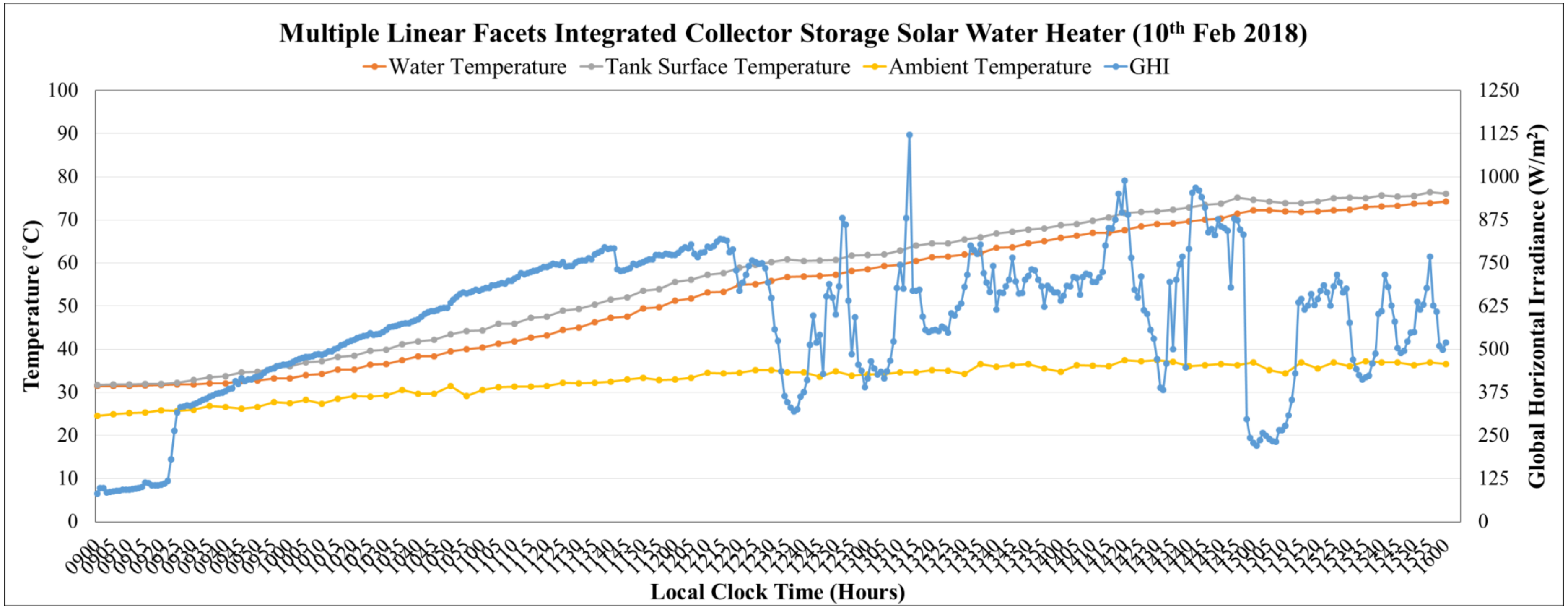

Figure 4.2: Measurement Results of Tank Surface Temperature, Water Temperature in the Storage Tank, Ambient Temperature and Global Solar Irradiance versus Local Clock Time on 10th Feb 2018

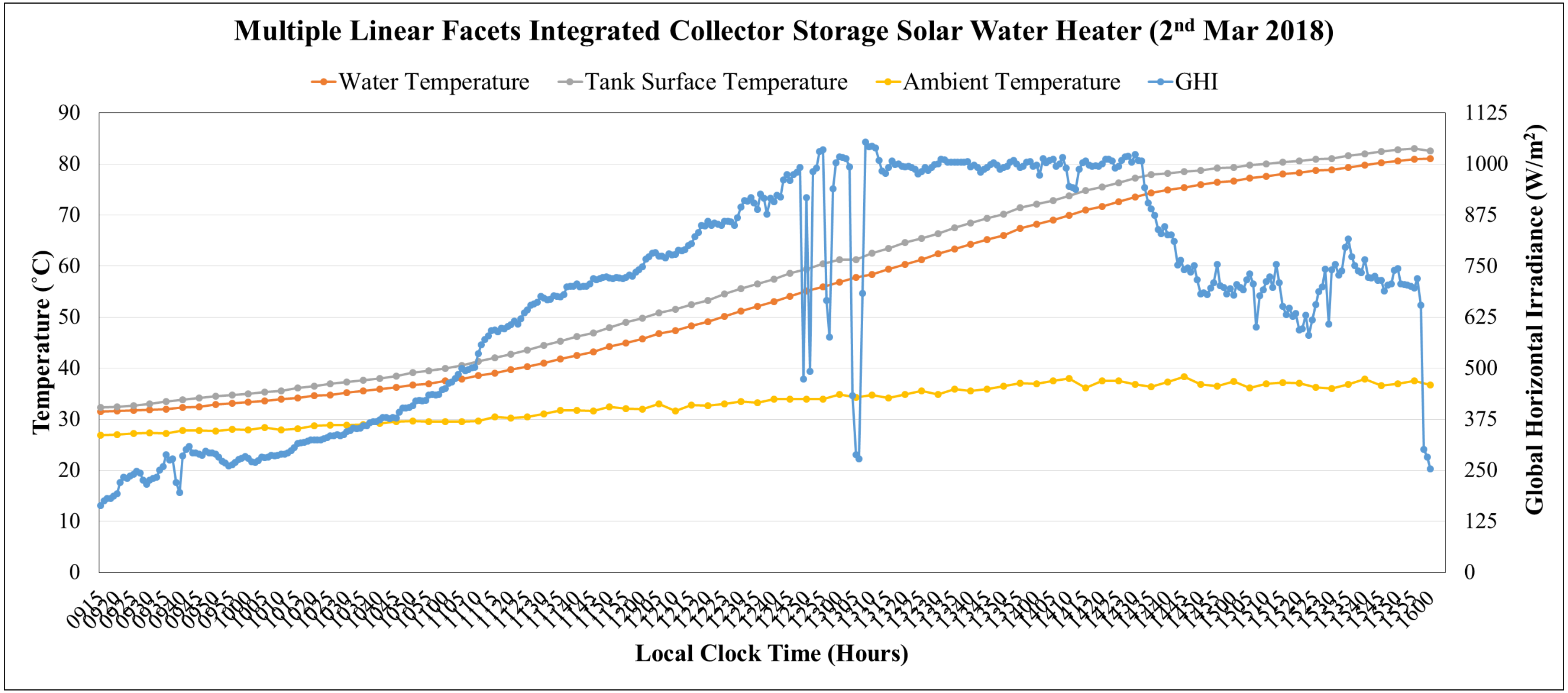

Figure 4.3: Measurement Results of Tank Surface Temperature, Water Temperature in the Storage Tank, Ambient Temperature and Global Solar Irradiance versus Local Clock Time on 2nd Mar 2018

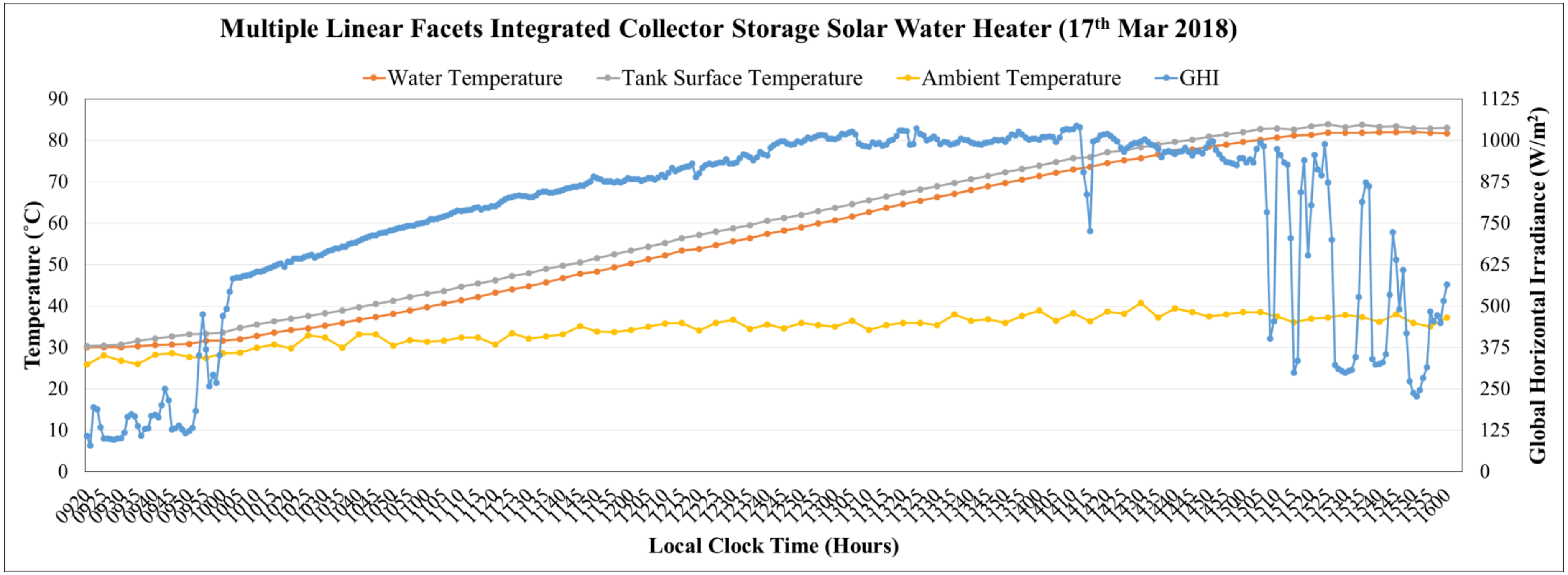

Figure 4.4: Measurement Results of Tank Surface Temperature, Water Temperature in the Storage Tank, Ambient Temperature and Global Solar Irradiance versus Local Clock Time on 17th Mar 2018

Based on the measurement results that shown in Fig. 4.1 to 4.4, the highest water temperature in the storage tank that can be achieved on 25th Jan 2018, 10th Feb 2018, 2nd Mar 2018 and 17th Mar 2018 are 61.0 °C, 74.2 °C, 83.0 °C and 82.2°C respectively. While the highest tank surface temperature that can be achieved on 25th Jan 2018, 10th Feb 2018, 2nd Mar 2018 and 17th Mar 2018 are 64.0 °C, 76.4 °C, 84.5 °C and 84.0 °C respectively. Besides that, there are also some common characteristics that shared by all of the measurement results. First of all, the temperature of the tank surface for all the measurement results were always higher than the temperature of water in the storage tank and there is always a gap in between these two temperatures. This is due to the solar radiation that radiated on the prototype will first heated up the tank surface and only then the heat gained was transfer to the water in the storage tank through natural convection. Besides that, when the global solar irradiance started to drop in the evening, the rate of increase for both tank surface and water temperatures were slowed down and the gap between them will be getting smaller. This is because the heat gained from the solar radiation is almost same as the heat loss to the surroundings due to the temperature differences between the prototype and the ambient, and hence the temperature for both the tank surface and water in the storage tank kept constant.

Table 4.1: The Specifications of the Multiple Linear Facets ICSSWH

Description	**Feature/Value**
Type of reflector	Low iron silver coating mirror
Dimension of each mirror at one side	- 83 mm (width) × 1000 mm (length) × 3 mm (thickness) - 122 mm (width) × 1000 mm (length) × 3 mm (thickness) - 103 mm (width) × 1000 mm (length) × 3 mm (thickness) - 65 mm (width) × 1000 mm (length) × 3 mm (thickness)
Total number of mirrors at one side	4
Inclined angle of each mirror	- 0° - 45.0° - 60.3° - 66.6°
Total reflective area of the collector	0.733 m^2
Dimension of glazing	1134 mm (length) × 618 mm (width) × 5 mm (thickness)
Dimension of absorber tank	150 mm (radius) × 1000 mm (length)

Area of the entry aperture	0.493 m^2
Total volume of water in the storage tank	17.67 L
Orientation of the prototype	Along east-west direction
Latitude	4.31 °N
Longitude	101.15 °E

In table 4.1, the specifications of the multiple linear facets ICSSWH prototype were shown. To further study the thermal performance of the prototype of the multiple linear facets ICSSWH system, the formulas that shown below were applied. The total amount of solar energy that radiated on the entry aperture of the prototype over a time interval can be computed by using

$$Q_{incident} = I_{ave} A \Delta t \tag{4.1}$$

where $Q_{incident}$ is the total amount of solar energy radiated on the entry aperture (J), I_{ave} is the average global solar irradiance (W/m^2), A is the total area of the entry aperture of the multiple linear facets ICSSWH (m^2) and Δt is the time interval (s). The area of the entry aperture of the prototype is 0.493m^2.

The total thermal energy that gained by the multiple linear facets ICSSWH can be calculated as

$$Q_{col} = m c_{water} (T_{f,\, heating} - T_{i,\, heating}) \tag{4.2}$$

where Q_{col} is the total thermal energy gained (J), m is the total mass of water in the storage tank (kg), c_{water} is the specific heat capacity of water (4184 J/kg. °C), $T_{i,\, heating}$ and $T_{f,\, heating}$ are the initial and final temperature of water in the storage tank (°C).

Hence, the system efficiency of the multiple linear facets ICSSWH by using Eq. 4.3,

$$\eta_{sys} = \frac{m c_{water} (T_{f,\, heating} - T_{i,\, heating})}{I_{ave} A \Delta t} \tag{4.3}$$

The thermal performance analysis of the multiple linear facets ICSSWH for different weather conditions is tabulated in Table 4.1 and a graph of system efficiency against $\Delta T/I_{ave}$ is plotted as shown in Figure 4.5 provided that

$$\Delta T = T_{ave,\, heating} - T_{ave,\, amb} \tag{4.4}$$

in which

$$T_{ave,\, heating} = \left(\frac{T_{i,\, heating} + T_{f,\, heating}}{2} \right) \tag{4.5}$$

and

$$T_{ave,\, amb} = \left(\frac{T_{i,\, amb} + T_{f,\, amb}}{2} \right) \tag{4.6}$$

where ΔT is the difference between average water temperature in storage tank and average ambient temperature, $T_{ave,\, heating}$ is the average temperature of water in the storage tank over a time interval, $T_{i,\, heating}$ and $T_{f,\, heating}$ are the initial and final water temperature in the storage tank within the time interval, $T_{ave,\, amb}$ is the average ambient temperature over a time interval, $T_{i,\, amb}$ and $T_{f,\, amb}$ are the initial and final ambient temperature within the time interval.

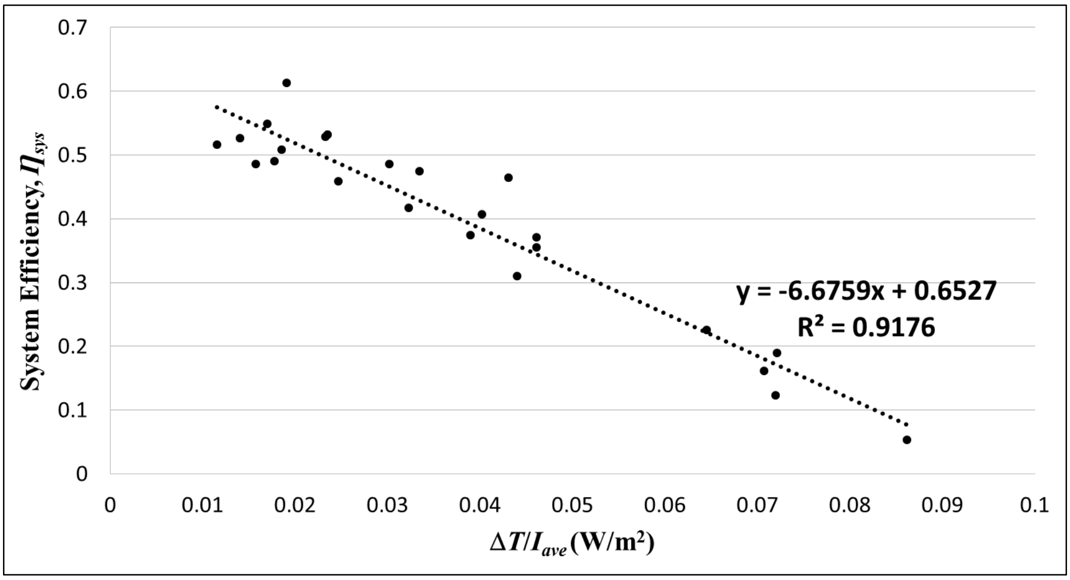

Figure 4.5: Graph of System Efficiency against $\Delta T/I_{ave}$

Based on the graph that displayed in Fig. 4.5, the y-intercept of the graph represents the theoretical highest system efficiency that can be achieved by the multiple linear facets ICSSWH which is 65.27 %. When comparing the highest system efficiency with the daily system efficiencies that achieved by the multiple linear facets ICSSWH in Table 4.1, it showed a difference between them and the different in efficiency is due to the loss of heat from the system to the environment. The value of the X-intercept of the graph in Fig.4.5 is 0.0978. By using the value of X-intercept and assume the average global solar irradiance to be 1000 W/m^2 with an ambient temperature of 28 °C, the theoretical highest water temperature in the storage tank that can be achieved will be 125.8 °C. Besides that, the graph in Fig. 4.5 also showed a linear relationship between the system efficiency and $\Delta T/I_{ave}$.

4.2 Economic Analysis of the Multiple Linear Facets ICSSWH System.

In order to evaluate the economic feasibility of the multiple linear facets ICSSWH system, the payback period of it can be computed with the following formulas:

$$n_{\text{pay}} = -\frac{\ln\left[1 - S_{\text{total}} i' / P_{\text{ann}}\right]}{\ln\left(1 + i'\right)} \tag{4.7}$$

in which

$$i' = \left(\frac{1+i}{1+j}\right) - 1 \tag{4.8}$$

where S_{total} is the total manufacturing cost of the multiple linear facets ICSSWH system, P_{ann} is the electricity cost saving per year (RM/year), i is the interest rate and j is the inflation rate.

For this project, let us consider an interest rate of 3% if a loan is made to build the multiple linear facets ICSSWH system with the capacity of 17.67 L or 17.67 kg water and the inflation rate is 4%. The daily energy consumption to heat up 17.67 kg of water from 25 °C to 83.0 °C is equal to 1.1911 kWh which means a daily net energy of 1.1911 kWH can be obtained from the multiple linear facets ICSSWH system. The net energy gained is equivalent to daily consumption of RM 0.3287 in the electric bill as the electricity unit cost in Malaysia is RM 0.276/kWh. Hence, the total electricity cost saving per year will be RM 120.00 if the multiple linear facets ICSSWH system is used to replace the electrical water heater. The breakdown cost for all the components that used to build the multiple linear facets ICSSWH system is shown in Table 4.2. Based on the table, the total cost for the construction of the whole system is RM 520.85. By using the Eq. 4.7, the total payback period obtained is 4.23 years in which it is considered quite profitable as most of the SWH can lasts for about 20 years.

Table 4.2: The Breakdown Cost for All the Components That Used to Build the Multiple Linear Facets ICSSWH System

Component	Description	Quantity	Unit Price (RM)	Retail Price (RM)
Piping System	½’’ VIP full bore ball valve (340)	2 units	11.50/unit	23.00
	½’’ G.I. elbow	1 unit	1.40/unit	1.40
	½’’ K.C. nipple	2 units	1.80/unit	3.60
	½’’ steam nipple	1 unit	2.60/unit	2.60
	8’’ × ½’’ G.I. Pipe	2 units	6.90/unit	13.80
	Seal tape	2 units	0.60/unit	1.20
Solar Collector	2 units of construction adhesive sealant	2 units	8.48/unit	16.96
	1unit of 1134 mm × 618 mm × 5 mm clear float glass	1 unit	42.40/unit	42.40
	732844 mm^2 of Mirror	732844 mm^2	$6.6 \times 10^{-5}/mm^2$	48.37
	3 units of Polyfoam	3 units	2.50/unit	7.50
	Plywood	2423734 mm^2	$2.07 \times 10^{-5}/mm^2$	50.17
	Screw (25pieces/packet)	1 packet	1.80/packet	1.80

Solar Collector (cont.)	Sealant silicone	2 units	7.10/unit	14.20
	Shellac	2 units	13.78/unit	27.56
	Single sided signage 284 mm × 618 mm material 3mm transparency acrylic sheet	2 units	39.00/unit	78.00
	1’’ × 2’’ × 980 mm timber strip	6 units	2.383/unit	14.30
Storage Tank	Black paint	2 units	5.90/unit	11.80
	150mm (6’’) G.I. pipe	1m	122.192/m	122.19
	200 mm × 190mm × 5mm metal plate	2 units	20.00/unit	40.00
			Total Retail Cost (RM)	**520.85**

CHAPTER 5

CONCLUSION AND RECOMMENDATIONS

In this project, the introduction of multiple linear facets collector into an integrated collector storage solar water heater (ICSSWH) system has proved that it can achieved the maximum system efficiency of 65.27 % and the highest water temperature in the storage tank of 83.0 °C on a sunny day. Besides that, the prototype of the system is easily constructed as its collector is made of different angles of facet mirrors and the materials that needed for other components are also easily obtained. Furthermore, the cost for the construction of the whole system is just RM 520.85 with a payback period of 4.23 years which is considered quite short as compared to other solar water heaters. Even though the system is already considered well-performed, but there are still some recommendations which can help to further improve the overall performance of the system.

Firstly, the angle on the supportive frame for the mirrors maybe slightly deviated from the actual angle that needed since it was manually made. Thus, inclinometer can be used to increase the accuracy of the angles on the supportive frame during the cutting process as well as when attaching the mirror onto the supportive frame. Next, the use of better thermal insulating materials to replace polyfoam as the insulation for the system and apply double glazing for the system will be able to enhance the heat retaining capability of the system especially during night time. Lastly, replacing the galvanized iron pipe with higher thermal conductivity materials such as copper, bronze and aluminium to act as the absorber tank will greatly improve the thermal performance of the system as the tank will be heat up faster and more heat will be transfer to the water.

REFERENCES

Chen, C.J., 2011. *Physics of Solar Energy*. New Jersry: John Wiley & Sons, Inc.

Chong, K.K., Chay, K.G. and Chin, K.H., 2012. Study of a Solar Water Heater using Stationary V-trough Collector. *Renewable Energy*, 39, pp. 207-215.

Devanarayanan, K. and Murugavel, K.K., 2014. Integrated collector storage solar water heater with compound parabolic concentrator – development and progress. *Renewable and Sustainable Energy Reviews*, 39, pp. 51 - 64.

Garnier, C., Currie, J. and Muneer, T., 2009. Integrated Collector Storage Solar Water Heater: Temperature Stratification. *Applied Energy*, 86, pp. 1465-1489.

Gertzos, K.P., Pnevmatikakis, S.E. and Caouris, Y.G., 2008. Experimental and Numerical Study of Heat Transfer Phenomena, inside a Flat-Plate Integrated Collector Storage Solar Water Heater (ICSSWH), with Indirect Heat Withdrawal. *Energy Conversion and Management*, 49, pp. 3104-3115.

Hamed, M., Fallah, A., Brahim, A.B., 2017. Numerical Analysis of Charging and Discharging Performance of an Integrated Collector Storage Solar Water Heater. *International Journal of Hydrogen Energy*, 42, pp. 8777-8789.

Johari, D., Yadav, A. and Verma, R., 2012. *Study of Solar Water Heaters Based On Energy Analysis.* In: Trends and Advances in Mechanical Engineering,YMCA University of Science & Technology, Faridabad, Haryana, Oct 19-20, 2012.

Kalogirou, S.A., 2004. Solar Thermal Collectors and Applications. *Progress in Energy and Combustion Science*, 30, pp. 231-295.

Kumar, R. and Rosen, M.A., 2010. Thermal Performance of Integrated Collector Storage Solar Water Heater with Corrugated Absorber Surface. *Applied Thermal Engineering*, 30, pp. 1764-1768.

Kumar, R. and Rosen, M. A., 2011. Integrated collector-storage solar water heater with extended storage unit. *Applied Thermal Engineering*, 31, pp. 348 - 354.

Laughton, C., 2010. *Solar Domestic Water Heating*. London: Earthscan.

Shelke,V.G., Patil, C.V. and Sontakke, K.R., 2014. Solar Water Heating Systems: A Review. *International Journal of Scientific Engineering and* Research, 3 (4), pp. 13-17.

Shukla, R., Sumathy, K., Erickson, P. and Jiawei, G., 2013. Recent Advances in the Solar Water Heating Systems: A Review. *Renewable and Sustainable Energy Reviews*, 19, pp. 173-190.

Smyth, M., Eames, P.C., and Norton, B., 2003. Heat Retaining Integrated Collector / Storage Solar Water Heaters. *Solar Energy*, 75, pp. 27-34.

Smyth, M., Eames, P.C. and Norton, B., 2006. Integrated Collector Storage Solar Water Heaters. *Renewable and Sustainable Energy Reviews*, 10, pp. 503-538.

Souliotis, M., Chemisana, D., Caouris, Y.G. and Tripanagnostopoulos, Y., 2012. Experimental study of integrated collector storage solar water heaters. *Renewable Energy*, 50, pp. 1083 - 1094.

Twidell, J. and Weir, T., 2015. *Renewable Energy Resources*. 3rd ed. New York: Routledge.

APPENDICES

Appendix A: Raw Experiment Data of 25th Jan 2018

Date	1/25/2018
Weather	Cloudy

T_1	Water Temperature
T_2	Tank Surface Temperature
T_3	Ambient Temperature

Time	GHI	T_1	T_2	T_3	Time	GHI	T_1	T_2	T_3	Time	GHI	T_1	T_2	T_3
0900					1200	721	40.5	44.2	30.6	1500	996	58.8	62.7	35.0
						708					847			
						726					952			
						761					756			
						773					567			
0905					1205	747	41.2	45.1	31.4	1505	525	59.4	62.8	34.6
						736					474			
						705					591			
						705					533			
						692					538			
0910					1210	702	41.9	45.9	31.4	1510	472	59.8	63.0	34.3
						699					452			
						646					603			
						667					879			
						712					900			
0915					1215	720	42.6	46.7	31.2	1515	570	60.0	63.5	34.2
						699					452			
						695					524			
						677					456			
						647					421			
0920					1220	630	43.3	47.3	31.0	1520	419	60.4	63.3	33.5
						633					601			
						636					702			
						631					789			

						611					727			
0925					1225	599	44.1	48.0	31.5	1525	666	60.8	64.0	34.2
						600					480			
						619					311			
						640					289			
						645					270			
0930					1230	606	44.7	48.6	31.8	1530	214	61.0	63.2	33.6
						595					285			
						588					200			
						601					194			
						657					148			
0935					1235	641	45.3	49.2	32.1	1535	137	61.0	62.7	32.2
						650					136			
						617					123			
						584					129			
						585					129			
0940					1240	597	46.0	49.8	32.0	1540	126	60.9	61.8	32.6
						590					123			
						609					127			
						607					138			
						608					155			
0945					1245	598	46.6	50.4	32.4	1545	164	60.8	61.2	32.2
						576								
						559								
						534								
						553								
0950					1250	575	47.2	50.9	31.7	1550				
						585								
						588								
						590								
						578								
0955					1255	576	47.8	51.4	31.6	1555				
						566								
						563								
						556								
						550								
1000					1300	532	48.4	51.8	31.3	1600				
						535								
						529								
						525								
						511								
1005					1305	506	49.0	52.2	31.8	1605				
						507								
						500								
						471								

						438								
1010	318	31.2	33.2	26.7	1310	421	49.5	52.5	32.1	1610				
	320					433								
	315					435								
	321					444								
	286					445								
1015	276	31.4	33.3	26.8	1315	451	49.9	52.8	31.0	1615				
	258					447								
	272					427								
	272					439								
	289					426								
1020	297	31.7	33.6	27.0	1320	404	50.3	53.0	31.9	1620				
	297					438								
	299					440								
	291					446								
	276					449								
1025	290	32.0	33.9	27.3	1325	447	50.7	53.3	32.0	1625				
	308					438								
	298					441								
	310					433								
	327					443								
1030	339	32.3	34.3	27.8	1330	460	51.0	53.6	31.8	1630				
	349					462								
	359					453								
	374					447								
	382					456								
1035	371	32.6	34.8	28.0	1335	453	51.5	54.0	32.0	1635				
	367					480								
	368					488								
	360					470								
	343					478								
1040	337	33.0	35.1	28.5	1340	482	51.9	54.4	32.0	1640				
	346					497								
	347					493								
	345					502								
	348					515								
1045	344	33.5	35.5	27.5	1345	507	52.3	54.9	32.4	1645				
	353					506								
	358					491								
	363					507								
	365					526								
1050	377	33.8	35.8	28.0	1350	561	52.7	55.3	32.1	1650				
	382					562								
	386					579								
	387					597								

	375					613								
1055	356	34.2	36.2	28.1	1355	617	53.2	56.0	32.1	1655				
	362					613								
	360					585								
	355					557								
	361					531								
1100	374	34.5	36.5	28.3	1400	497	53.6	56.2	32.5	1700				
	407					466								
	386					467								
	404					480								
	432					482								
1105	453	34.9	37.0	27.9	1405	485	54.0	56.5	32.0					
	462					530								
	499					542								
	508					550								
	529					627								
1110	548	35.3	37.7	28.0	1410	623	54.3	57.0	32.2					
	541					660								
	535					652								
	554					650								
	521					670								
1115	494	35.9	38.3	28.7	1415	671	54.8	57.7	33.2					
	518					682								
	527					689								
	526					722								
	463					714								
1120	462	36.4	38.9	28.8	1420	725	55.3	58.5	32.8					
	433					731								
	422					680								
	403					660								
	383					623								
1125	377	36.8	39.2	29.1	1425	639	56.0	59.2	33.0					
	374					674								
	346					644								
	324					532								
	322					506								
1130	324	37.1	39.4	28.8	1430	463	56.5	59.3	33.5					
	332					481								
	340					514								
	523					377								
	576					352								
1135	573	37.5	40.2	28.9	1435	358	56.8	59.3	32.9					
	591					475								
	595					491								
	573					487								

	560					466								
	566					450								
	579					421								
1140	582	37.9	40.9	29.3	1440	419	57.1	59.5	33.3					
	590					434								
	600					360								
	595					378								
	591					413								
1145	610	38.4	41.6	29.8	1445	460	57.2	59.5	32.9					
	630					530								
	640					501								
	609					479								
	592					703								
1150	657	39.0	42.4	29.5	1450	727	57.5	59.9	33.9					
	671					917								
	658					863								
	637					956								
	669					748								
1155	683	39.8	43.2	30.2	1455	831	58.0	61.4	33.6					
	651					934								
	682					913								

Appendix B: Raw Experiment Data of 10th Feb 2018

Date	2/10/2018
Weather	Partially Sunny

T_1	Water Temperature
T_2	Tank Surface Temperature
T_3	Ambient Temperature

Time	GHI	T_1	T_2	T_3	Time	GHI	T_1	T_2	T_3	Time	GHI	T_1	T_2	T_3
	82					774					228			
	97					780					221			
0900	98	31.4	31.7	24.6	1200	790	51.3	55.6	33.0	1500	236	72.2	74.7	37.0
	85					796					258			
	86					792					249			
	88					804					239			
0905	89	31.5	31.8	24.9	1205	777	51.8	56.1	33.4	1505	233	72.2	74.3	35.2
	90					767					232			
	92					780					265			

	92					781					265			
0910	93	31.5	31.8	25.2	1210	798	53.2	57.3	34.5	1510	278	72.0	73.9	34.4
	95					794					308			
	96					799					353			
	97					811					430			
	101					819					636			
0915	114	31.6	32.0	25.3	1215	818	53.3	57.6	34.4	1515	645	71.8	73.9	37.0
	112					815					615			
	105					782					627			
	105					790					660			
	106					728					628			
0920	107	31.7	32.0	25.8	1220	669	54.9	58.9	34.5	1520	646	72.0	74.3	35.5
	110					694					670			
	118					715					685			
	180					741					664			
	263					758					626			
0925	316	31.8	32.2	25.7	1225	753	55.1	59.5	35.2	1525	682	72.2	75.0	37.0
	333					748					715			
	334					749					694			
	337					735					664			
	335					694					676			
0930	340	31.8	32.8	26.0	1230	648	55.8	60.2	35.2	1530	577	72.4	75.1	36.0
	343					557					469			
	348					524					443			
	353					436					425			
	357					365					412			
0935	362	32.1	33.5	26.8	1235	346	56.7	60.8	34.6	1535	418	73.0	75.0	37.2
	366					330					423			
	370					319					459			
	372					326					488			
	374					362					603			
0940	378	32.1	33.7	26.6	1240	375	56.9	60.5	34.6	1540	610	73.1	75.7	37.0
	385					411					715			
	387					513					680			
	408					598					626			
	400					519					580			
0945	415	32.6	34.6	26.2	1245	542	57.0	60.6	33.6	1545	504	73.2	75.4	37.0
	408					428					489			
	412					653					495			
	413					688					522			
	419					650					548			
0950	421	32.7	34.8	26.6	1250	600	57.2	60.7	34.9	1550	549	73.8	75.6	36.3
	424					682					638			
	431					881					615			
	440					861					630			

	442					640					678			
0955	445 451 453 456 456	33.2	35.7	27.7	1255	485 592 456 438 390	58.1	61.8	33.9	1555	768 627 608 510 498	73.9	76.4	36.9
1000	458 463 468 471 475	33.3	36.0	27.5	1300	415 465 445 426 435	58.6	61.9	34.1	1600	519	74.2	76.0	36.5
1005	477 477 480 484 485	34.0	37.0	28.3	1305	415 437 467 523 678	59.3	62.0	34.2	1605				
1010	484 488 493 493 500	34.2	37.2	27.4	1310	745 676 880 1122 670	59.5	62.9	34.6	1610				
1015	504 511 515 521 524	35.3	38.2	28.5	1315	669 673 595 556 550	60.4	64.0	34.6	1615				
1020	527 532 535 539 540	35.3	38.5	29.2	1320	554 556 553 565 561	61.3	64.5	35.2	1620				
1025	547 542 543 545 550	36.4	39.6	29.0	1325	548 604 597 620 632	61.5	64.6	35.0	1625				
1030	556 564 566 568 571	36.6	39.9	29.3	1330	681 715 800 787 777	62.0	65.5	34.3	1630				
1035	574 575 576 580	37.5	41.1	30.6	1335	803 720 694 666	62.3	66.0	36.5	1635				

	583					742								
	587					615								
	595					664								
1040	602	38.3	41.8	29.7	1340	663	63.5	66.9	35.9	1640				
	607					683								
	611					702								
	611					766								
	614					696								
1045	618	38.4	42.2	29.6	1345	661	63.7	67.2	36.3	1645				
	620					663								
	620					702								
	635					712								
	644					732								
1050	652	39.5	43.5	31.4	1350	729	64.6	67.7	36.5	1650				
	660					701								
	664					683								
	661					623								
	664					684								
1055	668	40.0	44.2	29.1	1355	674	65.0	68.0	35.6	1655				
	672					664								
	670					665								
	674					641								
	678					655								
1100	678	40.4	44.3	30.5	1400	684	65.8	68.8	34.8	1700				
	685					683								
	686					710								
	689					707								
	692					659								
1105	691	41.3	45.9	31.2	1405	709	66.3	69.0	36.3					
	699					719								
	699					716								
	705					695								
	710					695								
1110	720	41.8	45.9	31.3	1410	708	67.0	69.8	36.2					
	717					724								
	721					800								
	723					852								
	727					850								
1115	728	42.7	47.3	31.3	1415	875	67.0	70.6	36.0					
	733					950								
	738					896								
	738					989								
1120	743	43.2	47.6	31.4	1420	890	67.6	71.6	37.5					
	748					765								
	746					672								

	744					651								
1125	752	44.5	48.9	32.2	1425	711	68.5	71.8	37.2					
	739					613								
	742					602								
	741					556								
	751					531								
1130	756	45.0	49.3	32.1	1430	471	69.0	71.9	37.5					
	757					388								
	757					382								
	763					459								
	761					695								
1135	775	46.3	50.4	32.2	1435	500	69.2	72.3	37.1					
	779					702								
	784					746								
	795					769								
	791					448								
1140	793	47.3	51.5	32.5	1440	791	69.6	72.8	36.0					
	793					954								
	732					968								
	727					961								
	728					941								
1145	732	47.6	52.0	33.0	1445	911	70.0	73.5	36.3					
	735					838								
	748					849								
	745					831								
	749					877								
1150	753	49.5	53.6	33.4	1450	857	70.3	73.8	36.6					
	757					851								
	761					843								
	761					679								
	773					878								
1155	774	49.7	54.0	32.9	1455	874	71.5	75.2	36.3					
	771					846								
	776					833								
	775					297								
	774					243								

Appendix C: Raw Experiment Data of 2nd Mar 2018

Date	2/3/2018
Weather	Sunny

T_1	Water Temperature
T_2	Tank Surface Temperature
T_3	Ambient Temperature

Time	GHI	T_1	T_2	T_3	Time	GHI	T_1	T_2	T_3	Time	GHI	T_1	T_2	T_3
						749					679			
						768					705			
0900					1200	773	45.7	49.8	32.0	1500	698	76.7	79.3	37.4
						782					692			
						783					717			
						774					731			
						774					707			
0905					1205	770	46.8	50.9	33.0	1505	601	77.2	79.8	36.2
						781					677			
						777					692			
						779					713			
						789					724			
0910					1210	788	47.4	51.5	31.6	1510	698	77.6	80.0	37.0
						790					754			
						800					710			
	164					805					652			
	176					822					632			
0915	181	31.5	32.3	26.9	1215	833	48.3	52.5	32.8	1515	647	78.0	80.4	37.2
	181					850					627			
	187					849					634			
	193					860					594			
	221					850					596			
0920	233	31.6	32.4	27.0	1220	855	49.1	53.3	32.7	1520	630	78.3	80.6	37.1
	230					852					580			
	236					850					618			
	240					860					656			
	248					860					688			
0925	243	31.8	32.7	27.2	1225	858	50.2	54.5	33.0	1525	700	78.8	80.9	36.3
	226					850					743			
	216					869					608			
	226					894					741			
0930	231	31.9	33.0	27.3	1230	911	51.2	55.6	33.5	1530	754	78.9	81.1	36.0
	234					909					728			
	251					918					739			

	260					905					796			
	288					889					817			
	276					927					773			
0935	278	32.0	33.5	27.2	1235	917	52.1	56.5	33.2	1535	752	79.3	81.6	36.8
	220					878					738			
	195					917					734			
	286					907					766			
	302					923					723			
0940	308	32.3	33.8	27.8	1240	919	53.0	57.5	34.0	1540	721	79.8	82.0	37.9
	293					961					725			
	292					974					715			
	290					960					715			
	287					974					689			
0945	297	32.5	34.2	27.8	1245	980	54.1	58.6	34.0	1545	704	80.3	82.4	36.6
	292					992					707			
	293					474					740			
	290					918					744			
	283					492					707			
0950	272	32.9	34.5	27.7	1250	982	55.1	59.4	33.9	1550	705	80.6	82.8	37.0
	268					990					704			
	261					1031					701			
	264					1035					697			
	270					666					719			
0955	277	33.1	34.7	28.0	1255	576	56.0	60.5	34.0	1555	654	80.9	83.0	37.5
	280					940					302			
	284					1003					282			
	280					1017					253			
	271					1016					250			
1000	270	33.4	35.0	27.9	1300	1014	56.9	61.3	34.9	1600	259	81.1	82.6	36.7
	274					993					606			
	283					433					703			
	281					289					676			
	283					278					724			
1005	287	33.6	35.3	28.4	1305	683	57.8	61.3	34.3	1605	757	80.8	82.6	35.3
	286					1054					743			
	287					1043					748			
	290					1044					741			
	290					1040					698			
1010	292	33.9	35.6	27.9	1310	1009	58.4	62.6	34.8	1610	702	81.2	83.2	37.2
	299					983					695			
	305					977					740			
	316					991					710			
1015	317	34.2	36.1	28.2	1315	1007	59.4	63.5	34.2	1615	329	81.6	83.5	36.6
	319					999					740			
	321					1001					720			

	325					995					734			
1020	324	34.6	36.5	28.7	1320	993	60.4	64.6	34.9	1620	719	81.9	83.8	37.5
	324					994					702			
	324					992					670			
	327					987					675			
	330					976					669			
1025	334	34.8	36.9	28.8	1325	982	61.3	65.4	35.6	1625	645	82.2	83.9	36.9
	334					991					636			
	337					984					632			
	335					991					630			
	338					999					631			
1030	345	35.2	37.3	28.8	1330	1000	62.4	66.4	34.9	1630	652	82.3	84.0	36.2
	347					1012					654			
	353					1011					667			
	352					1005					655			
	353					1005					623			
1035	359	35.6	37.6	29.0	1335	1005	63.3	67.5	35.9	1635	608	82.5	84.2	37.5
	359					1005					638			
	366					1004					629			
	369					1005					578			
	370					1006					606			
1040	373	35.9	38.0	29.2	1340	993	64.3	68.5	35.6	1640	604	82.6	84.2	37.5
	380					997					595			
	379					992					606			
	377					980					576			
	380					987					605			
1045	378	36.3	38.5	29.6	1345	991	65.2	69.4	35.9	1645	607	82.6	84.2	37.1
	393					999					627			
	403					1003					614			
	403					997					613			
	404					988					620			
1050	408	36.7	39.1	29.7	1350	992	66.0	70.2	36.5	1650	641	82.7	84.3	37.2
	420					994					603			
	421					1004					604			
	420					1009					594			
	421					1001					617			
1055	435	37.0	39.5	29.6	1355	991	67.4	71.5	37.1	1655	600	82.9	84.3	37.4
	436					995					618			
	435					1005					618			
	436					1006					604			
	448					994					624			
1100	451	37.5	40.0	29.5	1400	997	68.2	72.1	36.9	1700	628	83.0	84.5	37.4
	463					973								
	466					1013								
	475					1003								

	485					1009								
1105	500	37.9	40.6	29.5	1405	1012	69.0	72.9	37.5					
	494					995								
	496					1001								
	501					1016								
	503					990								
1110	536	38.6	41.3	29.7	1410	946	70.0	73.8	38.0					
	558					942								
	570					938								
	579					987								
	592					1003								
1115	594	39.0	42.0	30.5	1415	1008	71.0	74.8	36.2					
	590					997								
	598					995								
	597					996								
	603					995								
1120	607	39.7	42.8	30.2	1420	1000	71.7	75.5	37.5					
	616					1012								
	608					1012								
	621					1007								
	636					990								
1125	643	40.3	43.6	30.5	1425	995	72.6	76.3	37.5					
	654					1009								
	657					1018								
	661					1019								
	676					1005								
1130	672	41.0	44.5	31.0	1430	1024	73.5	77.2	36.8					
	668					1009								
	669					1008								
	677					942								
	676					905								
1135	674	41.8	45.3	31.8	1435	891	74.3	77.9	36.4					
	681					875								
	700					839								
	701					830								
	701					847								
1140	706	42.5	46.2	31.7	1440	827	74.9	78.2	37.3					
	699					827								
	701					811								
	701					753								
	707					765								
1145	720	43.2	46.9	31.6	1445	742	75.4	78.5	38.4					
	717					745								
	719					735								
	723					751								

	724					716								
	721					682								
	720					685								
1150	722	44.2	48.0	32.4	1450	681	76.0	78.8	36.8					
	721					696								
	719					710								
	723					755								
	728					702								
1155	725	45.0	49.0	32.1	1455	698	76.4	79.2	36.5					
	735					682								
	741					695								

Appendix D: Raw Experiment Data of 17th Mar 2018

Date	17/3/2018
Weather	Sunny

T_1	Water Temperature
T_2	Tank Surface Temperature
T_3	Ambient Temperature

Time	GHI	T_1	T_2	T_3	Time	GHI	T_1	T_2	T_3	Time	GHI	T_1	T_2	T_3
						883					947			
						883					934			
0900					1200	884	50.3	53.4	34.2	1500	943	79.6	82.0	38.6
						878					934			
						881					975			
						887					994			
						887					982			
0905					1205	881	51.3	54.3	35.1	1505	783	80.2	82.8	38.6
						888					402			
						896					455			
						890					974			
						903					956			
0910					1210	918	52.3	55.3	35.8	1510	933	80.7	82.9	37.5
						907					927			
						912					706			
						918					299			
0915					1215	921	53.4	56.5	35.9	1515	335	81.2	82.7	36.1
						922					844			
						930					941			

						889					653			
0920	108	30.1	30.3	25.9	1220	901	53.8	57.2	34.1	1520	805	81.4	83.4	37.0
	80					917					957			
	195					925					913			
	189					930					894			
	134					928					990			
0925	101	30.1	30.5	28.1	1225	930	54.8	58.0	35.9	1525	873	81.9	84.0	37.2
	100					933					701			
	99					934					323			
	98					944					311			
	101					930					305			
0930	102	30.1	30.7	26.8	1230	931	55.6	58.8	36.8	1530	299	81.9	83.2	37.9
	118					933					305			
	165					947					308			
	174					959					346			
	167					955					527			
0935	138	30.3	31.7	26.0	1235	950	56.5	59.6	34.5	1535	815	81.9	83.8	37.4
	109					940					874			
	130					950					862			
	132					965					340			
	169					959					324			
0940	172	30.6	32.2	28.3	1240	955	57.5	60.6	35.6	1540	326	82.0	83.3	36.2
	164					978					331			
	202					986					355			
	250					993					534			
	217					997					723			
0945	128	30.7	32.7	28.6	1245	998	58.3	61.3	34.6	1545	641	82.0	83.5	38.1
	131					991					490			
	139					988					610			
	128					990					418			
	117					998					273			
0950	123	30.9	33.2	27.8	1250	994	59.0	62.1	35.9	1550	237	82.2	82.9	36.0
	133					1000					228			
	184					1009					248			
	351					1005					283			
	475					1011					316			
0955	369	31.6	33.4	27.5	1255	1016	59.9	62.9	35.4	1555	484	81.9	82.9	35.0
	259					1017					455			
	293					1015					473			
	269					1005					450			
	351					1005					516			
1000	471	31.7	33.6	28.7	1300	1004	60.8	63.8	35.0	1600	565	81.8	83.0	37.3
	492					1008					550			
	544					1020					620			
	583					1019					608			

	586					1023					472			
1005	586	32.0	34.8	28.8	1305	1027	61.6	64.7	36.5	1605	395	81.9	82.9	37.6
	591					1018								
	593					991								
	595					984								
	600					983								
1010	604	32.8	35.6	29.9	1310	981	62.7	65.6	34.3	1610				
	604					994								
	607					990								
	613					993								
	616					985								
1015	620	33.6	36.4	30.8	1315	987	63.7	66.5	35.5	1615				
	626					999								
	629					1003								
	619					1014								
	633					1030								
1020	634	34.2	37.0	29.8	1320	1030	64.6	67.4	36.0	1620				
	644					1028								
	644					987								
	644					990								
	648					1037								
1025	652	34.7	37.7	32.9	1325	1020	65.4	68.2	36.0	1625				
	655					1015								
	647					1001								
	652					1006								
	655					1012								
1030	662	35.3	38.3	32.5	1330	1004	66.4	69.0	35.5	1630				
	667					990								
	670					996								
	674					994								
	675					987								
1035	680	35.9	39.0	29.9	1335	991	67.1	69.8	38.0	1635				
	680					994								
	687					1005								
	691					1002								
	692					1001								
1040	697	36.7	39.8	33.2	1340	994	68.0	70.6	36.5	1640				
	702					991								
	707					990								
	710					988								
	713					993								
1045	713	37.4	40.5	33.2	1345	994	68.9	71.5	36.9	1645				
	720					995								
	722					1003								
	724					1001								

	729					1003								
1050	730	38.2	41.3	30.5	1350	996	69.7	72.3	36.0	1650				
	733					1007								
	736					1018								
	738					1015								
	742					1027								
1055	743	39.0	42.2	31.8	1355	1018	70.5	73.1	37.7	1655				
	743					1008								
	748					1002								
	749					1006								
	751					1005								
1100	755	39.7	43.0	31.4	1400	1003	71.4	73.9	38.9	1700				
	762					1010								
	763					1011								
	764					1012								
	767					1011								
1105	771	40.6	43.7	31.6	1405	996	72.2	74.8	36.5					
	774					1008								
	779					1031								
	784					1035								
	788					1034								
1110	787	41.4	44.7	32.5	1410	1035	73.0	75.7	38.3					
	789					1044								
	790					1040								
	792					905								
	796					838								
1115	799	42.2	45.5	32.5	1415	727	73.7	76.0	36.3					
	792					998								
	796					1003								
	796					1015								
	802					1019								
1120	802	43.2	46.3	30.8	1420	1021	74.6	77.2	38.7					
	809					1013								
	817					1005								
	823					997								
	827					977								
1125	829	44.0	47.3	33.5	1425	967	75.2	77.6	38.2					
	832					978								
	834					987								
	833					993								
	832					993								
1130	830	44.8	48.0	32.2	1430	997	75.8	78.3	40.8					
	829					1004								
	834					995								
	843					987								

	845					985								
	846					975								
	843					950								
1135	843	45.8	49.0	32.7	1435	965	76.6	79.0	37.2					
	845					968								
	848					965								
	851					960								
	856					966								
1140	857	46.8	49.8	33.2	1440	968	77.2	79.7	39.5					
	861					978								
	861					966								
	863					955								
	863					968								
1145	870	47.8	50.6	35.2	1445	968	77.8	80.2	38.6					
	876					962								
	891					978								
	886					993								
	883					997								
1150	877	48.4	51.6	33.9	1450	972	78.5	80.9	37.5					
	876					958								
	877					945								
	874					936								
	876					934								
1155	873	49.4	52.5	33.7	1455	930	79.0	81.5	38.1					
	878					925								
	886					947								